EUMETSAT Satellite Application Facility on
Support to Operational Hydrology and Water Management

Algorithm Theoretical Baseline Document (ATBD) for product H14 – SM-DAS-2

Soil Wetness Index in the roots region

Version: 0.2
Date: 30 September2011

DOCUMENT CHANGE RECORD

Issue / Revision	Date	Description
0.1	16/05/2011	Draft version prepared for PCR
0.2	30/09/2011	Updates, acknowledging PCR Review Board comments.

Algorithm Theoretical Baseline Document ATBD-14
Product SM-DAS-2
Soil Wetness Index in the roots region

INDEX

Acronyms

AMSU	Advanced Microwave Sounding Unit (on NOAA and MetOp)
AMSU-A	Advanced Microwave Sounding Unit - A (on NOAA and MetOp)
AMSU-B	Advanced Microwave Sounding Unit - B (on NOAA up to 17)
ATDD	Algorithms Theoretical Definition Document
AU	Anadolu University (in Turkey)
BfG	Bundesanstalt für Gewässerkunde (in Germany)
CAF	Central Application Facility (of EUMETSAT)
CDOP	Continuous Development-Operations Phase
CESBIO	Centre d'Etudes Spatiales de la BIOsphere (of CNRS, in France)
CM-SAF	SAF on Climate Monitoring
CNMCA	Centro Nazionale di Meteorologia e Climatologia Aeronautica (in Italy)
CNR	Consiglio Nazionale delle Ricerche (of Italy)
CNRS	Centre Nationale de la Recherche Scientifique (of France)
DMSP	Defense Meteorological Satellite Program
DPC	Dipartimento Protezione Civile (of Italy)
EARS	EUMETSAT Advanced Retransmission Service
ECMWF	European Centre for Medium-range Weather Forecasts
EDC	EUMETSAT Data Centre, previously known as U-MARF
EUM	Short for EUMETSAT
EUMETCast	EUMETSAT’s Broadcast System for Environmental Data
EUMETSAT	European Organisation for the Exploitation of Meteorological Satellites
FMI	Finnish Meteorological Institute
FTP	File Transfer Protocol
GEO	Geostationary Earth Orbit
GRAS-SAF	SAF on GRAS Meteorology
HDF	Hierarchical Data Format
HRV	High Resolution Visible (one SEVIRI channel)
H-SAF	SAF on Support to Operational Hydrology and Water Management
IDL©	Interactive Data Language
IFOV	Instantaneous Field Of View
IMWM	Institute of Meteorology and Water Management (in Poland)
IPF	Institut für Photogrammetrie und Fernerkundung (of TU-Wien, in Austria)
IPWG	International Precipitation Working Group
IR	Infra Red
IRM	Institut Royal Météorologique (of Belgium) (alternative of RMI)
ISAC	Istituto di Scienze dell’Atmosfera e del Clima (of CNR, Italy)
ITU	İstanbul Technical University (in Turkey)
LATMOS	Laboratoire Atmosphères, Milieux, Observations Spatiales (of CNRS, in France)
LEO	Low Earth Orbit
LSA-SAF	SAF on Land Surface Analysis
Météo France	National Meteorological Service of France
METU	Middle East Technical University (in Turkey)
MHS	Microwave Humidity Sounder (on NOAA 18 and 19, and on MetOp)
MSG	Meteosat Second Generation (Meteosat 8, 9, 10, 11)
MVIRI	Meteosat Visible and Infra Red Imager (on Meteosat up to 7)
MW	Micro Wave
NESDIS	National Environmental Satellite, Data and Information Services
NMA	National Meteorological Administration (of Romania)
NOAA	National Oceanic and Atmospheric Administration (Agency and satellite)
NWC-SAF	SAF in support to Nowcasting & Very Short Range Forecasting
NWP	Numerical Weather Prediction
NWP-SAF	SAF on Numerical Weather Prediction
O3M-SAF	SAF on Ozone and Atmospheric Chemistry Monitoring
OMSZ	Hungarian Meteorological Service
ORR	Operations Readiness Review
OSI-SAF	SAF on Ocean and Sea Ice
PDF	Probability Density Function

PEHRPP	Pilot Evaluation of High Resolution Precipitation Products
Pixel	Picture element
PMW	Passive Micro-Wave
PP	Project Plan
PR	Precipitation Radar (on TRMM)
PUM	Product User Manual
PVR	Product Validation Report
RMI	Royal Meteorological Institute (of Belgium) (alternative of IRM)
RR	Rain Rate
RU	Rapid Update
SAF	Satellite Application Facility
SEVIRI	Spinning Enhanced Visible and Infra-Red Imager (on Meteosat from 8 onwards)
SHMÚ	Slovak Hydro-Meteorological Institute
SSM/I	Special Sensor Microwave / Imager (on DMSP up to F-15)
SSMIS	Special Sensor Microwave Imager/Sounder (on DMSP starting with S-16)
SYKE	Suomen ympäristökeskus (Finnish Environment Institute)
T_{BB}	Equivalent Blackbody Temperature (used for IR)
TKK	Teknillinen korkeakoulu (Helsinki University of Technology)
TMI	TRMM Microwave Imager (on TRMM)
TRMM	Tropical Rainfall Measuring Mission UKMO
TSMS	Turkish State Meteorological Service
TU-Wien	Technische Universität Wien (in Austria)
U-MARF	Unified Meteorological Archive and Retrieval Facility
UniFe	University of Ferrara (in Italy)
URD	User Requirements Document
UTC	Universal Coordinated Time
VIS	Visible
ZAMG	Zentralanstalt für Meteorologie und Geodynamik (of Austria)

1 The EUMETSAT Satellite Application Facilities and H-SAF

The "*EUMETSAT Satellite Application Facility on Support to Operational Hydrology and Water Management (H-SAF)*" is part of the distributed application ground segment of the "*European Organisation for the Exploitation of Meteorological Satellites (EUMETSAT)*". The application ground segment consists of a "*Central Application Facility (CAF)*" and a network of eight "*Satellite Application Facilities (SAFs*)" dedicated to development and operational activities to provide satellite-derived data to support specific user communities. See ***Fig. 01***.

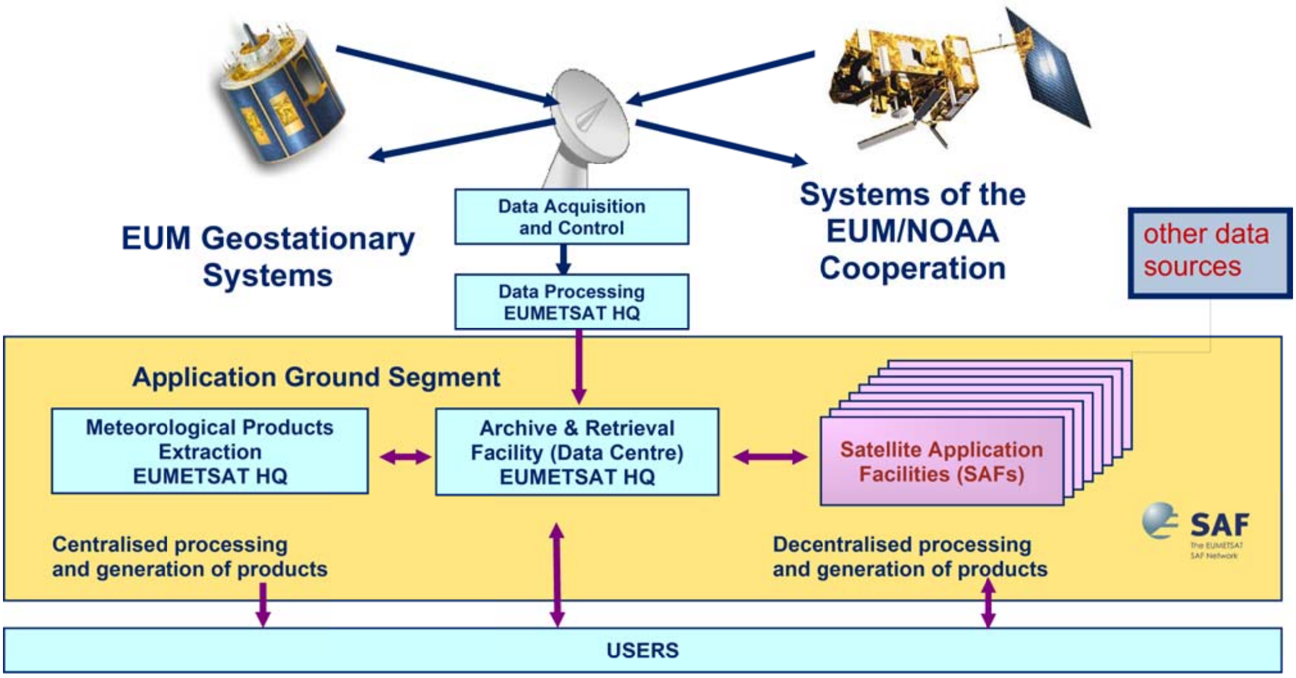

Fig. 01 - Conceptual scheme of the EUMETSAT application ground segment.

Fig. 02 reminds the current composition of the EUMETSAT SAF network (in order of establishment).

NWC SAF	OSI SAF	O3M SAF	CM SAF	NWP SAF	GRAS SAF	LSA SAF	H SAF
Nowcasting & Very Short Range Forecasting	Ocean and Sea Ice	Ozone & Atmospheric Chemistry Monitoring	Climate Monitoring	Numerical Weather Prediction	GRAS Meteorology	Land Surface Analysis	Operational Hydrology & Water Management

Fig. 02 - Current composition of the EUMETSAT SAF network (in order of establishment).

The H-SAF was established by the EUMETSAT Council on 3 July 2005; its Development Phase started on 1st September 2005 and ends on 31 August 2010. The list of H-SAF products is shown in ***Table 01.***

Acronym	Identifier	Name
PR-OBS-1	H-01	Precipitation rate at ground by MW conical scanners (with indication of phase)
PR-OBS-2	H-02	Precipitation rate at ground by MW cross-track scanners (with indication of phase)

Acronym	Identifier	Name
PR-OBS-3	H-03	Precipitation rate at ground by GEO/IR supported by LEO/MW
PR-OBS-4	H-04	Precipitation rate at ground by LEO/MW supported by GEO/IR (with flag for phase)
PR-OBS-5	H-05	Accumulated precipitation at ground by blended MW and IR
PR-OBS-6	H-15	Blended SEVIRI Convection area/ LEO MW Convective Precipitation
PR-ASS-1	H-06	Instantaneous and accumulated precipitation at ground computed by a NWP model
SM-OBS-2	H-08	Small-scale surface soil moisture by radar scatterometer
SM-OBS-3	H-16	Large-scale surface soil moisture by radar scatterometer
SM-DAS-2	H-14	Liquid root zone soil water index by scatterometer assimilation in NWP model
SN-OBS-1	H-10	Snow detection (snow mask) by VIS/IR radiometry
SN-OBS-2	H-11	Snow status (dry/wet) by MW radiometry
SN-OBS-3	H-12	Effective snow cover by VIS/IR radiometry
SN-OBS-4	H-13	Snow water equivalent by MW radiometry

2 Introduction to product SM-DAS-2

2.1 *Principle of the product*

In the framework of the H-SAF project, an advanced surface data assimilation system is being developed at ECMWF to retrieve root zone soil moisture profile index from ASCAT surface soil moisture index (CAF product). This product inherits from the previous volumetric product of the development phase, SM-ASS-1. In contrast to SM-ASS-1, SM-DAS-2 is produced by a specific production chain which is being developed by ECMWF for H-SAF. Its production is based on a Simplified Extended Kalman Filter (SEKF).

This product consists of NRT **liquid root zone soil water content index** from assimilation of the global CAF **surface soil moisture index** product (H-16, SM-OBS-3) in the ECMWF H-TESSEL Land Surface Model. ECMWF generates SM-DAS-2 (Liquid Root zone soil moisture), thereafter ZAMG disseminates the products.

In the soil moisture assimilation system, the surface observation from ASCAT is propagated towards the roots region down to 2.89 m below surface, providing estimates for 4 layers (thicknesses 0.07, 0.21, 0.72 and 1.89 m). The ECMWF model generates soil moisture profile information according to the Hydrology Tiled ECMWF Scheme for Surface Exchanges over Land (HTESSEL) (see Fig. 03).

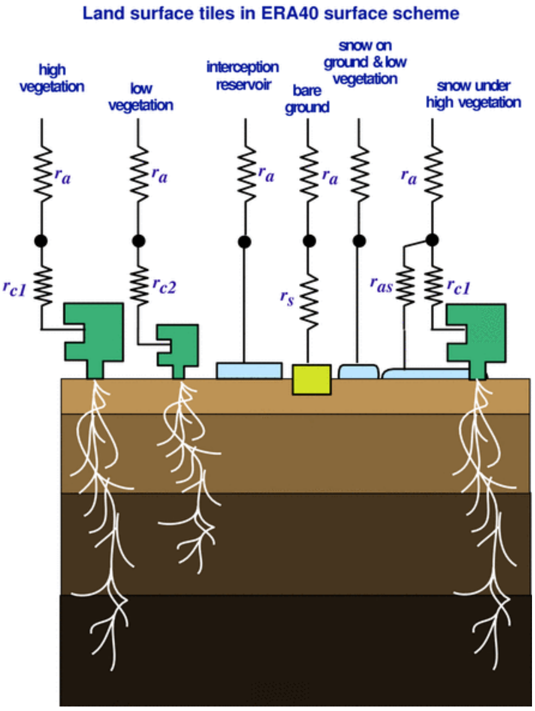

Fig. 03 - Hydrology Tiled ECMWF Scheme for Surface Exchanges over Land (HTESSEL).

The assimilation scheme constrains the 24-hour forecast of soil moisture on any point of the Gaussian grid to be as close as possible to all observations.

SM-DAS-2 is produced in a continuous way in order to ensure the time series consistency of the product (and also to provide values when there is no satellite data, from the model propagation).

2.2 *Main operational characteristics*

The *horizontal resolution (Δx)*. The effective resolution is driven by SM-DAS-2 production chain resolution which is ~ 25 km. For land surfaces processes are resolved on a discret grid which determines the effective soil moisture product resolution. The discret grid is a Gaussian reduced grid at T799. Conclusion:

- horizontal resolution: Δx ~ 25 km.

The *vertical resolution*. The soil moisture profile is computed for four layers: surface to 7 cm, 7 cm to 28 cm, 28 cm to 100 cm, and 100 cm to 289 cm.

The *observing cycle (Δt)*. The SM-DAS-2 product is produced daily at 00UTC, based on assimilation of the global CAF surface soil moisture index product (H-16, SM-OBS-3) in the ECMWF H-TESSEL Land Surface Model. Although the ASCAT CAF product observing cycle over European latitudes is ~ 36 h, the assimilation process leading to the SM-DAS-2 product has its own time evolution. The product is outputted at 24-hour intervals, thus:

- observing cycle: Δt ~ 24 h

The *timeliness (δ)*. For a continuous assimilation process it is difficult to identify the time lag between the observation and the product output. By considering the time needed by the model to "digest" soil moisture observation, the SM-DAS-2 timeliness will be:

- timeliness δ ~ 36 h.

The *accuracy* is completed by temporal correlation against ground measurements which validates the accuracy of the product in terms of temporal variability. SM-DAS-2 is evaluated *a-posteriori* by means of the validation activity. See section 5 "Examples of SM-DAS-2 product".

2.3 Architecture of the products generation chain

The architecture of the SM-DAS-2 product generation chain is shown in ***Fig. 04***. The figure includes mention of the primary source of satellite data, the Global surface soil moisture product generated by EUMETSAT and disseminated via EUMETCast.

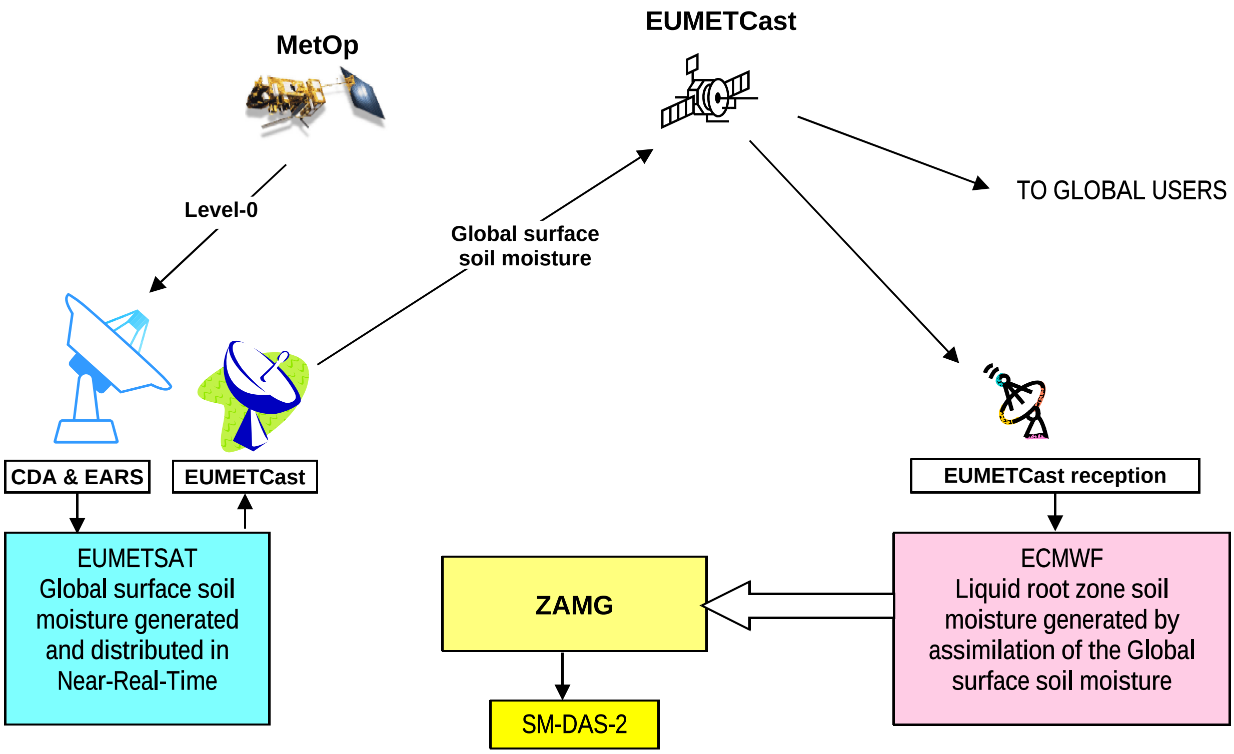

Fig. 04 - Conceptual architecture of SM-DAS-2 production chain.

The figure shows that ECMWF produces SM-DAS-2 that is addressed to ZAMG for further dissemination in the H-SAF community.

2.4 Product development team

Names and references of the main participants for SM-DAS-2 algorithm development and integration are listed in following table:

European Centre for Medium-Range Weather Forecasts (ECMWF)	Patricia de Rosnay (Leader)	patricia.rosnay@ecmwf.int
	Clément Albergel	clement.albergel@ecmwf.int
	Lars Isaksen	lars.isaksen@ecmwf.int

3 Processing concept

3.1 Short description of the ECMWF model

The generation of SM-DAS-2 inherits from the previous volumetric product of the development phase, SM-ASS-1. In contrast to SM-ASS-1, SM-DAS-2 is produced by a specific production chain which is being developed by ECMWF for H-SAF. It is processed from assimilation of the global CAF surface soil moisture index product (H-16, SM-OBS-3) and other observations in the ECMWF NWP model. The relationships between satellite data and output products are shown in ***Fig. 05***.

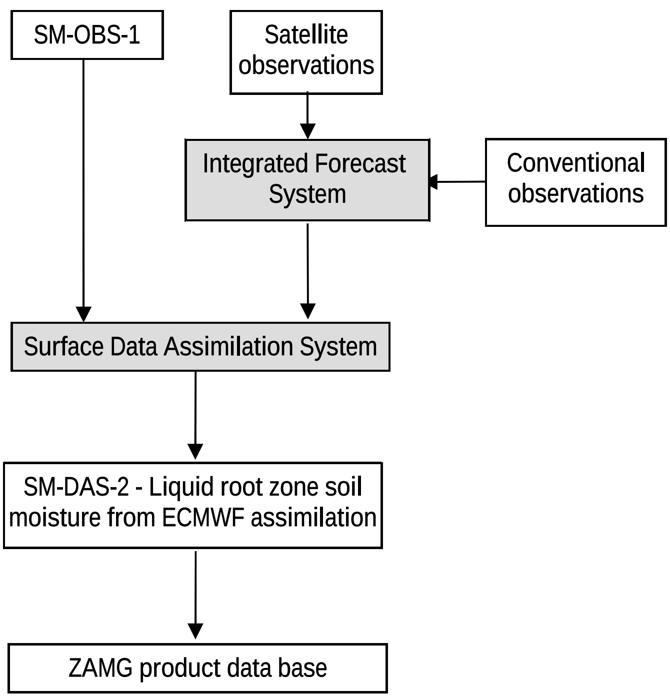

Fig. 05 - Soil moisture assimilation product generation chain.

The SM-DAS-2 production chain is operated at T799 spectral resolution, which corresponds for the land surface discret grid to grid point horizontal resolution of ~ 25 km. The atmospheric variables at each grid point comprise wind, temperature, humidity, ozone, cloud water and ice, cloud fraction, and also surface pressure. The model is integrated with a time step of 15 minutes.

In the model, clouds are generated by large-scale ascent, cumulus convection, boundary layer turbulence, and radiative cooling. Cloud fraction and cloud water/ice contents are forecast with their own prognostic equations. Interaction between clouds and radiation is based on radiative transfer computations for overcast and clear sky conditions. At ECMWF, global atmospheric analyses are produced at 00, 06, 12, and 18 UTC by two 4D-Var minimisation cycles running from 09 to 21 UTC and 21 to 09 UTC. Ten-day forecasts are issued twice a day from the 00 and 12 UTC analyses. For a detailed description of the forecast system the reader is referred to ECMWF 2003 and Haseler 2004.

The Hydrology Tiled ECMWF Scheme for Surface Exchanges over Land (HTESSEL; Balsamo et al. 2009, Van den Hurk et al. 2000, Viterbo and Beljaars 1995) is used in the SM-DAS-2 production chain. In contrast to SM-ASS-1, SM-DAS-2 production chain relies on the very last version of HTESSEL, which accounts for vegetation Leaf Area Index seasonal cycle and for an improved bare soil evaporation parameterization (Balsamo et al., 2011, Boussetta et al., 2011). The soil is discretized in four layers of 0.07, 0.28, 0.72, and 2.89 m depths (from top to bottom). The soil heat transfer is described through the Fourier law of diffusion. It is assumed that heat fluxes are predominantly vertical and that the effects of phase changes in the soil and the heat transfer associated with vertical movement of water can be neglected (De Vries 1975). At the bottom, no heat flux of energy is assumed, while at the top, the boundary condition is the soil heat flux at the surface area weighted over the tiles. The volumetric heat capacity is assumed to be constant; the heat conductivity is given by a combination of the values for the dry and the saturated heat conductivity, which is parameterized through the heat conductivity of the soil matrix and the thermal conductivity of water (Peters-Lidard et al. 1998).

Vertical movement of water in the unsaturated zone is computed using the Richards equation and Darcy's law. Functional relationships between the hydraulic conductivity and diffusivity and soil water are specified according to van Genuchten 1980. Values for soil moisture parameters are summarized in ***Table 03***.

Table 03 - Values of the volumetric soil moisture in Van Genuchten at saturation, field capacity, and permanent wilting point. Last column shows the plant available soil moisture. Units are in m^3/m^3.

Texture	Saturation	Field Capacity	Wilting Point	Available Water
Coarse	0.403	0.244	0.059	0.185
Medium	0.439	0.347	0.151	0.196
Medium-Fine	0.430	0.383	0.133	0.251
Fine	0.520	0.448	0.279	0.170
Very Fine	0.614	0.541	0.335	0.207
Organic	0.766	0.663	0.267	0.396

HTESSEL uses the dominant soil texture class for each gridpoint. This information is taken from the FAO (FAO, 2003) Soil types (***Fig. 06***) are derived from the FAO/UNESCO Digital Soil Map of the World, DSMW (FAO, 2003), which exists at a resolution of 5'x5' (about 10 km). FAO DSMW provides the information on two levels of soil depth namely 0-30 cm and 30-100 cm. Since the root zone is most important for the water holding, the 30-100 cm layer is selected for H-TESSEL. To interpolate to model target resolution, the dominant soil type is selected. This procedure has the advantage of preserving hydraulic properties when moving across various model resolutions (Balsamo et al., 2009). The climate eld used by the model has an index from 1 to 7 corresponding to the soil textures (see Fig. 10.26): 'coarse' (1),'medium' (2), 'medium ne' (3), 'ne' (4), 'very ne' (5), 'organic' (6), and 'tropical organic' (7).

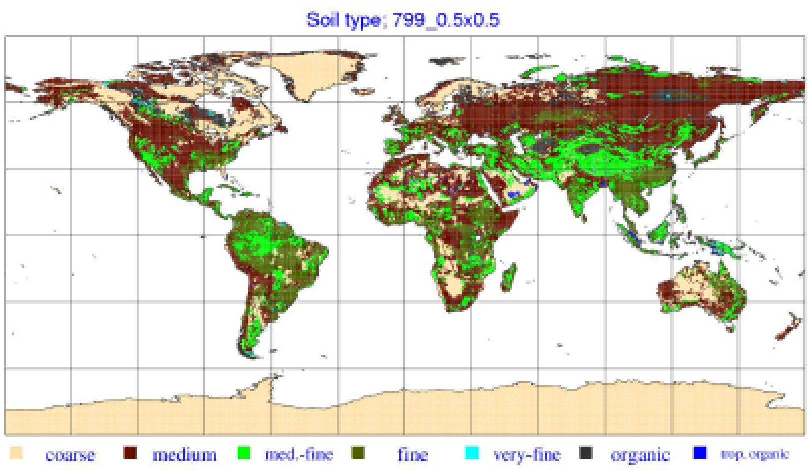

Fig. 06 - Soil type classes as used in H-TESSEL.

Each grid box in the model is divided in up to 8 vegetation tiles (bare ground, low and high vegetation without snow, exposed snow, snow under high vegetation, interception reservoir, ocean/lakes, and sea ice). In each grid box two vegetation classes (high and low) are present. Twenty vegetation types, including deserts, ice caps, inland water and ocean, have been defined from an external data base (USGS 1999). Each vegetation type is characterized by a set of fixed parameters for the minimum canopy resistance, spatial coverage, and leaf area index, a sensitivity coefficient describing the dependence of the canopy resistance on water vapour deficit, and the root distribution over the soil layers. The fraction of a grid box covered by each of the tiles depends on the type and relative area of low and high vegetation, and the presence of snow and intercepted water.

A skin temperature forms the interface between the soil and the atmosphere. It is calculated for each of the grid box tiles separately by solving the surface energy balance assuming a complete coverage of the specific tile. A resistance parameterization, which is different for each tile, is used to obtain the turbulent sensible and latent heat fluxes. The turbulent exchange coefficients may vary from tile to tile because of differing atmospheric stability, which is based on a Monin-Obukhov formulation. The model roughness lengths for momentum and heat / moisture are calculated for each grid box from fixed climatological fields as a blend of three contributions: vegetation, urbanization and orography. These 'effective' values represent the effects on turbulent transport of small-scale surface elements to subgrid orography. Although the surface is tiled, energy and water budgets are evaluated for a single atmospheric and soil profile per grid box. The archived fluxes for a grid box are area weighted averages as derived from the individual tiles. Further details on the surface-atmosphere coupling are given in (ECMWF 2008).

3.2 *The liquid root zone soil moisture processing chain (SM-DAS-2)*

The liquid root zone soil moisture product is of high interest for the hydrological community. Liquid root zone soil moisture is a key component of the continental water budget, it controls land surface fluxes and partition of precipitation into evapotranspiration and runoff. For operational hydrology applications root zone soil moisture is required to quantify accurately river routing, and reliability of flood prediction models strongly rely on accurate root zone soil moisture estimates. The SM-DAS-2 product is the first global product of consistent surface and root zone soil moisture available NRT for the NWP, climate and hydrological communities.

This product accomplishes the interest of the hydrological community since liquid root zone soil moisture is a key parameter for ETR estimation and for the hydrological applications for a large range of applications: initialization, validation, water budget computation, trend studies...

At high and mid latitudes the phase changes of water in the soil have an important effect on the water and energy transfer in the soil. As a matter of fact it is of importance to have a proper consideration of the liquid phase only.

The liquid root zone soil moisture product to be generated at ECMWF (see flow chart in ***Fig. 07***) is the result of a data assimilation process. The input consists of the large-scale global surface soil moisture product generated at EUMETSAT (‘observation’; see Section 3) and modelled root zone soil moisture (‘first guess’). The output from the land surface data assimilation is a statistically optimal product conditioned by the general characteristics of the ECMWF model.

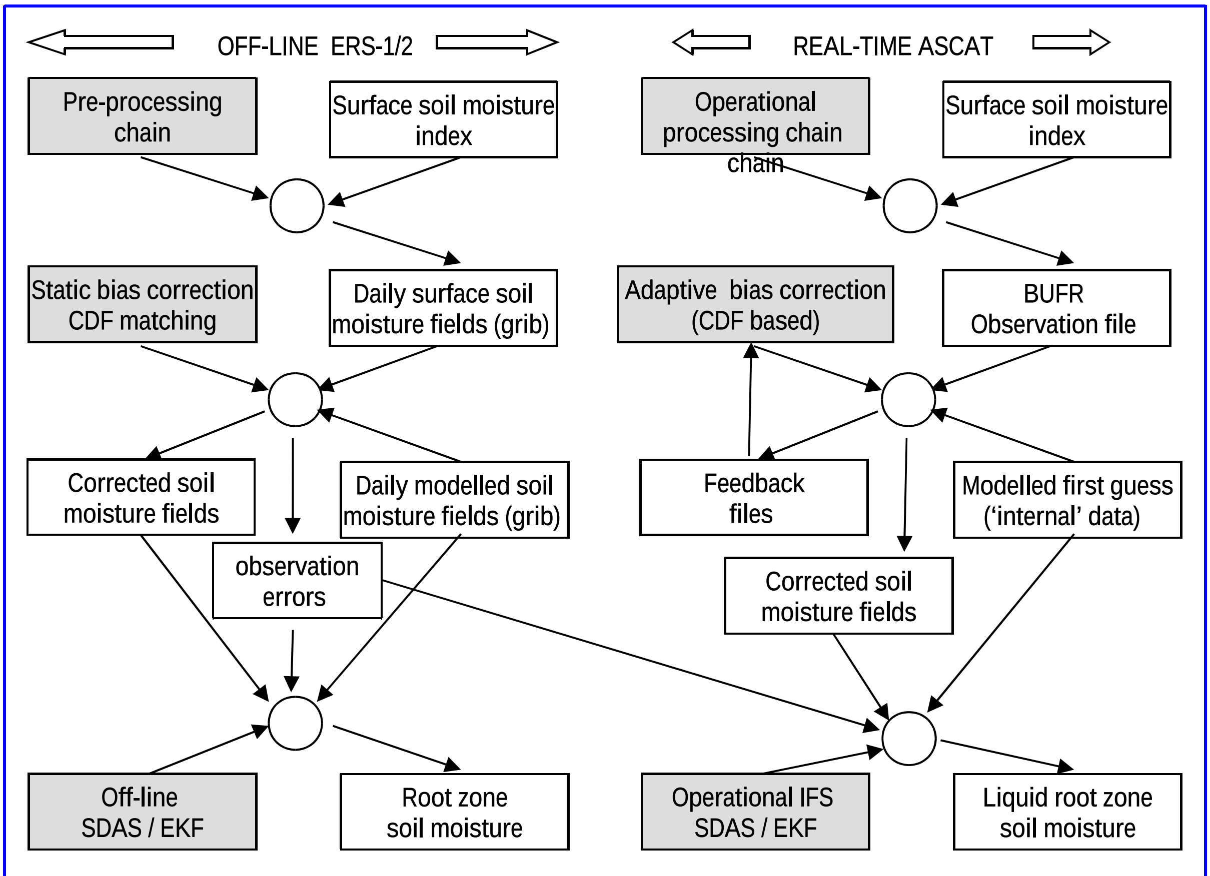

Fig. 07 - Flow chart of the liquid root zone soil moisture processing chain.

To integrate the satellite based observations in the forecast system, ERS and ASCAT swath based data sets are archived in BUFR format. For developing the observation operators, daily composite soil moisture images were also archived in GRIB format.

In any assimilation system based on linear estimation theory, systematic differences between the modelled first guess and the observations prevent a statistically optimal analysis and therefore have to be corrected (Dee and da Silva 1998). In the case of soil moisture, systematic differences between the model and the satellite derived surface soil moisture data are due to: (1) the terrestrial water balance equation depends on the temporal change of soil moisture. Consequently, every model has its own soil moisture climatology with a dynamical range defined through the wilting point and field capacity (Koster and Milly 1997). (2) Microwave observations in the frequency range from 5 GHz to 11 GHz represent the upper most soil layer with a depth of up to 0.02 m. In contrast, most operational hydrological models have a surface layer of between 0.05 to 0.10 m depth. The thin surface layer monitored by the satellite instrument will show a larger dynamical range and a different probability density function of soil moisture representing a faster dry down compared to models with a relatively thicker layer. Observations operators is needed to remove the systematic differences between satellite-derived soil moisture and the modelled first guess. For this application, Reichle and Koster 2004, and Drusch et al. 2005 explored the concept of Cumulative Distribution Function (CDF) matching.

To use the ASCAT data in the IFS Scipal et al. 2008a developed a CDF-matching between ERS and ERA-40 data sets (section 4). CDF-matching coefficients were then computed at several resolutions as shown in de Rosnay 2009 and used for SM-ASS-1. In the H-SAF CDOP, the CDF-matching approach was completely revised. As described in the next section, the SM-DAS-2 CDF-matching relies on forced land surface model simulation accounting for precipitation errors and using the last version of the land surface model H-TESSEL. In addition the revised CDF-matching is dynamic in time allowing accounting for seasonal cycle corrections.

The Land Surface analysis is part of the current forecast system: The early - delivery suite is operating with two 12-hour 4DVar atmospheric analyses using observations from 21:01 to 9:00 UTC and 9:01 to 21:00 UTC. The 10-day medium-range forecasts are initialized by two short cut-off 6-hour 4DVar analyses covering the periods from 21:01 to 3:00 UTC and 9:01 to 15:00 UTC. The surface analysis includes a soil moisture analysis based on an extended Kalman filter (EKF) using a 12-hour assimilation window, implemented in operations at ECMWF in 2010 (de Rosnay et al. 2011). The EKF is a variational assimilation system characterized by a model error that depends on the weather regime. Observations can be used at any time within the data assimilation window. In the near real time configuration, the 09 UTC to 21 UTC analysis window uses observations from 09 UTC to 21 UTC and produces the soil moisture analyses at 12 and 18 UTC.

The analysed soil moisture fields are available globally on a reduced Gaussian grid with horizontal spacing of ~ 23 km. The vertical resolution of the soil moisture profile is given through the four model layers of 0.07 m, 0.21 m, 0.72 m and 1.89 m thickness.

The generation of liquid root zone soil moisture is based on the assimilation of ASCAT Soil Moisture index in the ECMWF surface scheme, part of Integrated Forecasting System Data Assimilation system. SM-DAS-2 is produced offline by an early delivery suite at T799 using the EKF surface analysis in which screen level parameters and ASCAT data are assimilated. A prototype of SM-DAS-2 root zone soil moisture profile index was produced for July 2008-August 2010 (using IFS cycles 35r2 to 36r3). From September 2010, SM-DAS-2 is produced using IFS and H-TESSEL cycle 36r4.

4 Algorithms description

The key components in any data assimilation process are the first guess (i.e. modelled soil moisture), the observations (i.e. ERS / ASCAT derived surface soil moisture) and the data assimilation system itself. A short introduction to the operational numerical weather prediction model has been given in section 3.1; details on the satellite observations can be found in PUM-09. This section focus on the assimilation scheme, which comprises observation quality control, the observation operator, the Extended Kalman Filter (EKF).Purely technical processing steps, e.g. de- and encoding to GRIB and BUFR, will not be described in this document.

4.1 Observation quality control

Soil moisture retrieval from active microwave data is subject of certain limitations. Soil moisture can not be retrieved if the signal is dominated by scattering from dense vegetation, open water, rough topography or a snow covered/frozen land surfaces. To avoid assimilating data contaminated by these effects a rigorous quality check is carried out before the ERS/ASCAT data is assimilated (based on ASCAT product flags, Bartalis et al., 2007). A dynamic data masking is based on advisory and quality flags attached to the ERS/ASCAT level 2 soil moisture product and on analysed variables of the Land Surface Data Assimilation system. For details of the masking see ***Table 04.***. Using snow analysis conditions and two-meter air temperature conditions makes the mask dynamic. This is well illustrated in Fig. 8, which shows that masked areas in white, are more extended in Siberia and North America in March than in October.

Table 04 - Masking of data during the quality assurance, reference data and thresholds

Mask	Reference	Threshold
Open Water	ASCAT Level 2 advisory flag on open water	15 %
Rough Topography	ASCAT Level 2 advisory flag on topography	20 %
Vegetation	ASCAT Level 2 quality flag on sensitivity	< 2 dB
Noise	ASCAT Level 2 quality flag on sm error	> 0.07
Snow	Snow Analysis	snow is present
Soil Freezing	Screen level parameter Analysis	2 m Temp. < 273.15 K

a) *Mean dynamical mask for the first two weeks of March 2010*

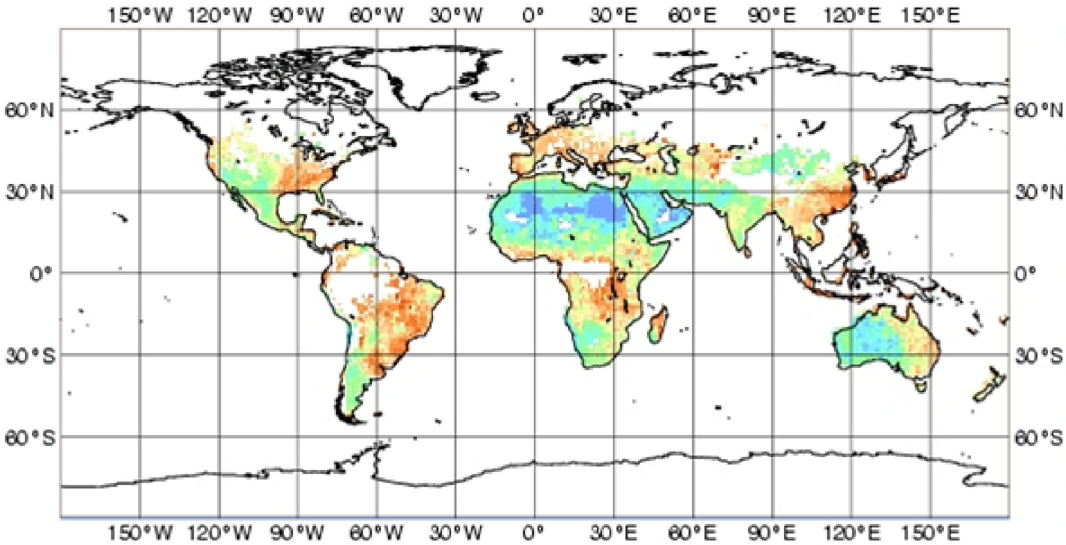

b) Mean dynamical mask for the firsat two weeks of October 2010

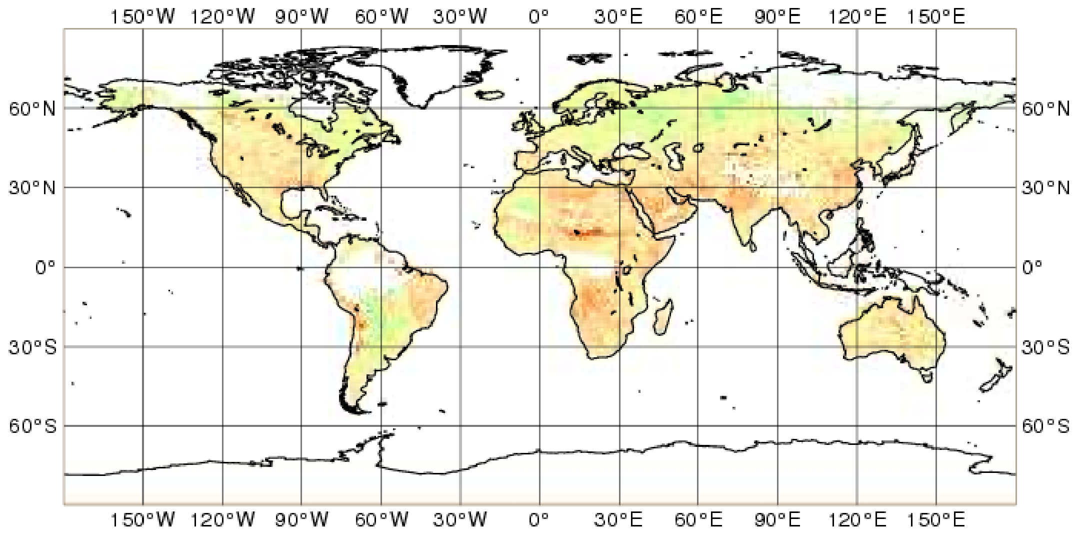

Fig. 8 - ECMWF dynamical mask (white areas) as illustrated by monitoring results in March 2010 (top) and October 2010 (bottom).

4.2 Observation operators / static bias correction

Generally, observation operators transform the modelled quantities into observed quantities. In the case of satellite observations, the observation operator is often a radiative transfer model that computes radiances or brightness temperatures from the modelled atmospheric fields. That is not the case here. In our application, a satellite derived soil moisture index (ranging from 0 to 1) representing the top millimetres of the soil is merged with modelled volumetric soil moisture for the top 7 cm layer. The observation operator developed and used to produce SM-ASS-1 converted the dimensionless index into a volumetric soil moisture (Scipal et al. 2008). In addition, systematic differences introduced through different (spatial and vertical) resolutions and the model's hydrological parameters had to be minimized.

Practical solutions to this problem are statistically derived transfer functions, which implicitly minimize the bias.

Since the operational assimilation of satellite derived soil moisture is a new topic for numerical weather prediction Centres, knowledge on the corresponding observation operators is limited. In this context, CDF matching was first introduced by Reichle and Koster 2004 and Drusch et al. 2005. Conceptually, the satellite derived data are scaled so that the CDFs of both data sets match (***Fig. 09***) and:

$$cdf_m(x') = cdf_s(x) \quad .$$

where cdf_s and cdf_m are the CDFs of the satellite derived soil moisture and the corresponding model data, respectively, and x and x' are the original and transformed satellite data. Technically, the two data sets (modelled soil moisture and observations) have to be ranked. Consecutively, the differences in soil moisture between the corresponding elements of each ranked data set will be computed. The observation operator, which removes the systematic differences between both data sets, is a polynomial fit to the ranked observed soil moisture values and the corresponding differences.

The entire ERS-1/2 data sets covering the period from 1992 to 2000 and the corresponding ERA40 re-analyses were used to develop the ASCAT data CDF matching to ECMWF soil moisture (Scipal et al., 2008). CDF matching and the subsequent polynomial fitting were performed using individual time series for each grid box. Comparing the individual coefficients resulted in a parameterized form of transfer functions that depend on selected hydro-climatological quantities. Soil maps were used to adjust the observation operator to be used with TESSEL or H-TESSEL depending on the IFS cycle used to assimilate ASCAT data. .

Assuming that ASCAT reflects the degree of saturation, model equivalent volumetric soil moisture can be derived by a rescaling with the model value of porosity, which is a prescribed quantity. However, such a transformation does not account for shortcomings of the model physics and the satellite retrieval method, which can result in large biases especially in the mean and variance. Therefore, we transform ws with respect to the climatology of the model. To this end soil moisture data from ERA-40 from the period 1992-2000 were used. The transformation was accomplished by scaling ASCAT soil moisture so that the cumulative distribution functions (CDF) of ASCAT and ERA-40 match. In similar studies, (Drusch et al. 2005; Drusch 2007), the data transformation was achieved by ranking datasets of satellite derived and model soil moisture and fitting a 3rd order polynomial to the differences. This approach corrected the differences in the mean, the variance, the skewness and the kurtosis. Here, we simplified the CDF matching to a linear transform. This effectively removes the differences in the first two moments (mean and variance). Differences in higher-order moments are mainly found in dry climates. In these regions, ERA is more skewed towards dry values and shows a narrower distribution (i.e. a higher kurtosis). This higher-order difference enters the assimilation as an uncorrected bias. The impact of ignoring differences in higherorder moments is nevertheless small and scarcely reaches values larger than 0.02 m^3/m^3. The disadvantage of neglecting differences in higher moments is, however, compensated by the robustness of the method especially in data sparse regions. The linear approach is also attractive as it can be fully parameterised by the mean and variance of ERA and ASCAT soil moisture. As described in Scipal et al. 2008, the transformed soil moisture index is then expressed as:

$$\Theta_{\hat{S}} = a + b \times \Theta_S \qquad (2)$$

In Eq. 2 denotes the transformed soil moisture and the ASCAT/ERS level 2 soil moisture. The intercept a and the slope b is calculated according to Eq.3 and Eq.4

$$a = \overline{\Theta}_M - \overline{\Theta}_S \cdot \frac{VAR(\Theta_M)}{VAR(\Theta_S)} \quad (3)$$

$$b = \frac{VAR(\Theta_M)}{VAR(\Theta_S)} \quad (4)$$

Where stands for soil moisture and the subscript S and M for satellite and model respectively. VAR denotes the variance and the bar denotes the mean of the respective sample.

Intercept a, and slope b are local coefficients, which were derived for each ERA40 model grid box. Global maps of intercept a and slope b are given in ***Fig. 9. These matching coefficients were used in the data assimilation chain of the H-SAF development phase SM-ASS-1 product.***

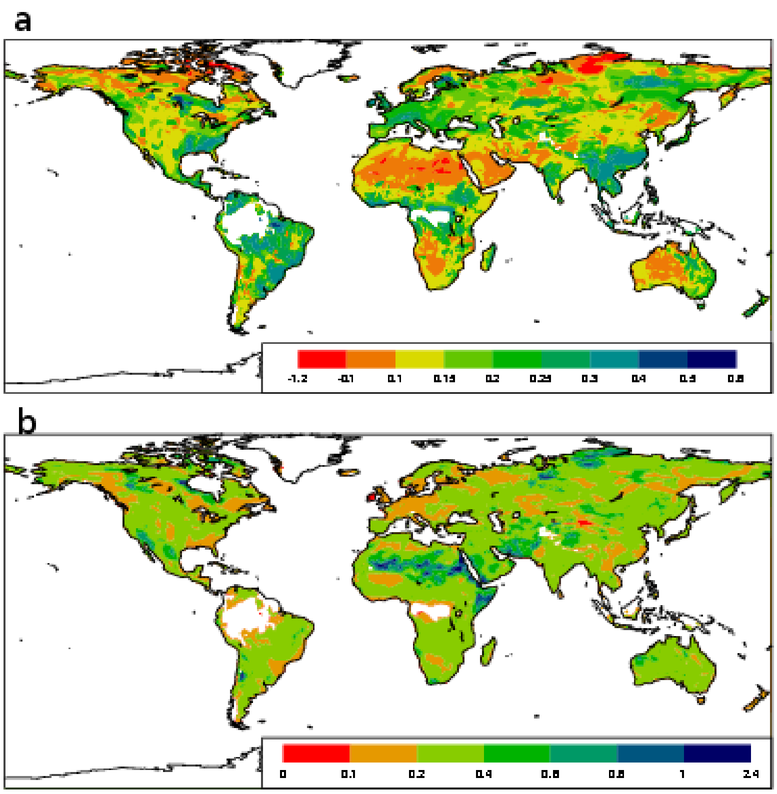

Fig. 9 - ASCAT CDF matching parameters used in the IFS at the 23 km resolution to convert ASCAT soil moisture index into volumetric soil moisture. Top panel represents the slope a and bottom panel shows the intercept b, both expressed in m3/m3 (from de Rosnay 2009).

4.3 Adaptive bias correction / observation monitoring

4.3.1 Improved EUMETSAT CAF ASCAT product since 18 August 2011

The EUMETSAT CAF ASCAT SSM product was improved since 18 August 2011. It is based on an improved backscatter calibration and an improved soil moisture retrieval algorithm. SSM is retrieved from the ASCAT backscatter measurements using a time series-based change detection approach previously developed for the ERS-1/2 scatterometer by Wagner et al. (1999) and recently improved by Naemi et al. (2009). The improved product is obtained by processing four years (January 2007-December 2010) of 25 km ASCAT backscatter measurements by deriving the change detection model parameters from the analysis of ASCAT time-series of 2007-2008 period. In fact, these model parameters are found slightly different from those derived from ERS-1/2 scatterometer time-series due to difference among ERS-1/2 and ASCAT sensors on both the spatial resolution and the absolute calibration of backscattering coefficient (Hahn and Wagner, 2011). The new ASCAT product is a crucial component of the SM-DAS-2 production chain. Figure 10 shows the ASCAT CAF product content with the old and new algorithm. The new ASCAT CAF product makes a better usage of the quality flag (in particular the noise filetring and processing flags), as described in de Rosnay et al., 2011a,c.

a) Old EUMETSAT CAF ASCAT product
(Operationally released before 18 August 2011)

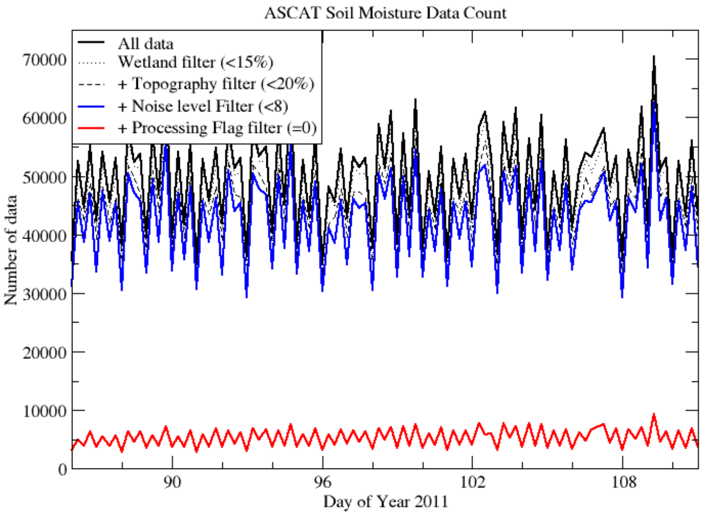

b) New improved EUMETSAT CAF ASCAT product
(Operationally released from 18 August 2011)

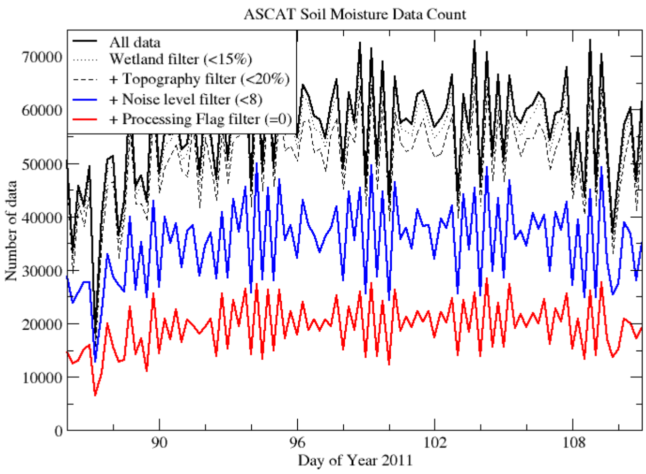

Figure 10: EUMETSAT CAF ASCAT surface soil moisture product data content and count (per 6 hours) for the test period (27 March 2011 - 21 April 2011), for (a) the ASCAT old operational product (CAF product until 18 August 2011), (b) the ASCAT new operational product that released on 18 August 2011. The black line shows the total soil moisture data count per 6 hour, the dotted-black line shows the data count after data from pixels with wetland fraction larger than 15% is rejected. The dashed line is the count after removing data from pixel with a topographic complexity larger than 20%. A noise level quality control (noise level ¡ 8) is applied resulting to the blue line. The ASCAT soil moisture data is used only when the processing flag is set zero, ensuring that the data is not corrupted. The total soil moisture data count available after quality control is the red line.

4.3.2 Motivations to revise the ASCAT CDF-matching for SM-DAS-2

Monitoring and assimilation of ASCAT surface soil moisture (SSM) data relies on a Cumulative Distribution Function (CDF) matching approach which rescales, for each model grid point, the scatterometer SSM index to fit the model SSM climatology. ASCAT CDF matching is based on (i) the ERS scatterometer (ERS/SCAT) data base, which provides a long data set consistent with ASCAT data, and (ii) the ERA-Interim soil moisture for 1992-2000 (Scipal et al., 2008). In CDOP, a revision of the ASCAT soil moisture bias correction approach is proposed, as was suggested in de Rosnay et al. (2011b) and devloped in de Rosnay et al. (2011a). The revised CDF matching is part of the SM-DAS-2 production chain and it will be use for operational monitoring from IFS cycle 37r3 (already in operational test suite at ECMWF). It still relies on ERS/SCAT data for 1992-2000. However it matches ERS/SCAT surface soil moisture CDF to that of the recent version of the ECMWF land surface model H-TESSEL. H-TESSEL climatology was obtained from offline simulations forced by ERA-Interim corrected by GPCP (Global Precipitation Climatology Project) Balsamo et al. (2011, 2010). The revised ASCAT CDF matching accounts for a seasonal cycle correction.

CDF matching transforms ASCAT normalised surface soil moisture index into model equivalent volumetric surface soil moisture. For the H-SAF development phase and the SM-ASS-1 product, the CDF matching parameters were derived for each model grid point from the CDF matching moments (mean and variance) of ERS/SCAT soil moisture data and ERA-Interim surface soil moisture for 1992-

2000. They were rescaled from TESSEL to H-TESSEL to account for soil texture dependent soil moisture ranges in H-TESSEL. This CDF matching is referred to as CDF1.
A first impact demonstration of ERS/SCAT soil moisture data assimilation using a nudging scheme was performed by Scipal et al. (2008). They showed that compared to the Optimum Interpolation soil moisture analysis (using screen level data), assimilating ASCAT data was slightly degrading the forecast scores. They recommended to use ASCAT data in an Extended Kalman Filter (EKF) analysis to account for observation errors and to combine ASCAT data with screen level proxy information. ASCAT soil moisture data assimilation in the EKF soil moisture analysis was shown to have a neutral impact on soil moisture and screen level parameters analysis and forecasts (de Rosnay et al. , 2011b). The impact of ASCAT data assimilation was limited by the quality of the ASCAT product, using non-appropriate processing and noise level flags as shown in the previous section, which was reducing considerably the number and the quality of data used in the analysis. In addition a large angular bias of ASCAT soil moisture was shown in de Rosnay (2009), resulting in rejecting data at large incidence angles and reducing further the amount of data available for data assimilation. An other issue was related to the main assumption in CDF1, which is that the systematic differences between observations and model are stationary. There are actually potentially large differences in the seasonal cycles of the ASCAT and ECMWF soil moisture. In a previous study, Draper et al. (2009) showed that for the AMSRE (Advanced Microwave Scanning Radiometer) SSM data and the M´et´eo-Frances Aire Limite ´ee Adaptation Dynamique développement InterNational (ALADIN) SSM, it is crucial to account for seasonal correction in the CDF matching. Not accounting for seasonal discrepancies between observations and model climatologies might affect the matching at both short time scale and seasonal scale.

Major modifications were implemented in November 2010 in the land surface model in IFS cycle 36r4 (Balsamo et al. , 2011). The bare soil evaporation parameterisation was improved by removing the lower wilting point limit for bare soil areas and by accounting for Lea Area Index seasonal cycle (Balsamo et al. , 2011; Boussetta et al. , 2011). These modifications had a significant impact on the soil moisture range (Albergel et al. , 2011). So, the TESSEL to H-TESSEL CDF moments rescaling used in CDF1 is not any longer valid from H-TESSEL cycle 36r4. Limitations in the CDF matching, important changes in H-TESSEL and improvement of the ASCAT CAF product justify a revision of the ASCAT soil moisture CDF matching for both the SM-DAS-2 production chain and for ASCAT operational monitoring at ECMWF.

4.3.3 ASCAT CDF-matching used in the SM-DAS-2 production chain

For SM-DAS-2, the CDF matching matches ERS/SCAT SSM climatology to that of ECMWF (HTESSEL cycle 36r4) for 1992-2000. ECMWF soil moisture climatology was generated offline in 2011, covering the period 1989-2009, using atmospheric forcing obtained from ERA-Interim corrected by Global Precipitation Climatology Project (GPCP) product (Balsamo et al. 2010). So, that the reference model climatology used for the improved CDF matching is much less affected by precipitation errors than the old CDF matching. The revised CDF matching is referred to as CDF2 in the following of this memorandum.
In addition to CDF2, a further improved CDF matching was investigated, by correcting for the seasonal cycle differences between ASCAT and ECMWF SSM climatologies. It is referred to as CDF2 seasonal. CDF2 seasonal was computed separately for each month, using a three month moving window, based on the 1992- 2000 ERS/SCAT and H-TESSEL cycle 36r4 climatologies.

For all the CDF matching approaches described above, moments are computed based on observations and model SSM values in snow free and for two-meter air temperature above 0 degrees C (in the model). CDF moments are computed at the ERA-Interim resolution (ie 80km). They are interpolated to each resolution the SM-DAS-2 resolution (25km). CDF matching coefficients are then computed at the SM-DAS-2 resolution from interpolated moments. The revised CDF matching approaches (without and with seasonal correction) were applied to rescale the ASCAT 2009 improved test data set provided by EUMETSAT. Rescaled ASCAT SSM data was compared to H-TESSEL cycle 36r4 SSM for 2009.

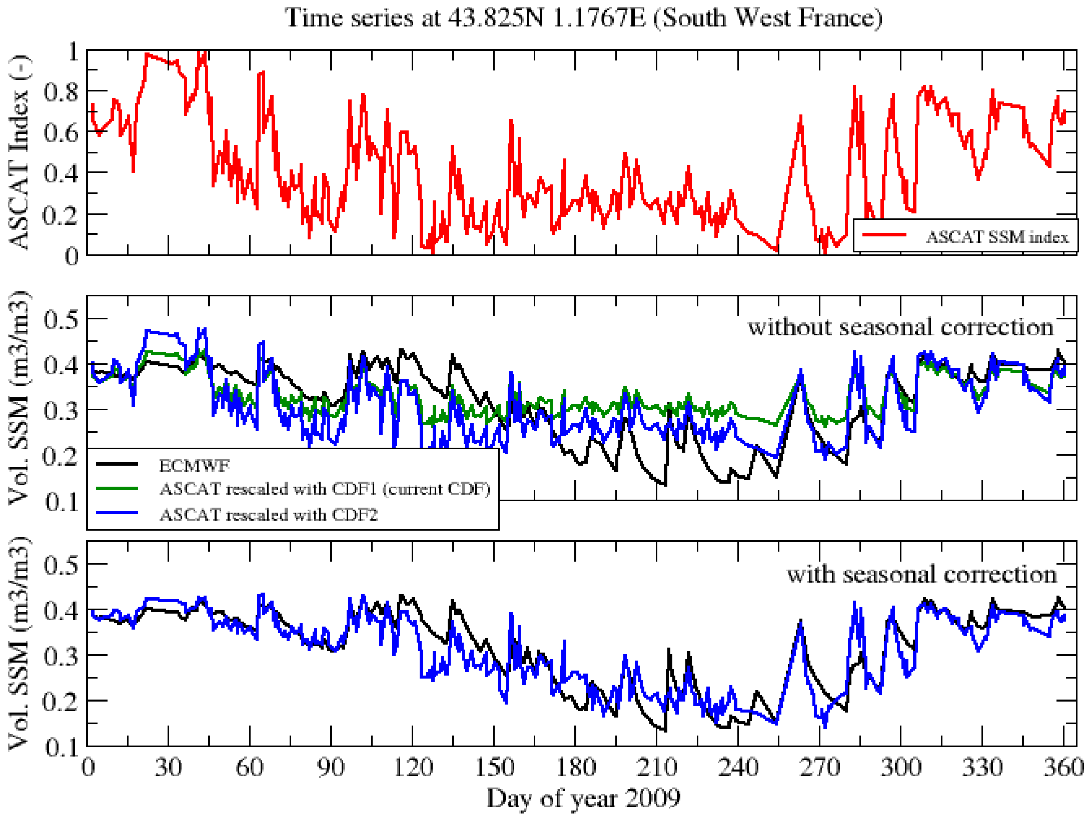

Figure 11: Surface soil moisture time series for 2009, for one location in South West of France, for ASCAT data (top) and for ECMWF (H-TESSEL cycle 36r4) and ASCAT data rescaled without (middle) and with (bottom) seasonal cycle correction.

	Min	Max	Mean	StD
ECMWF (m^3m^{-3})	0.066	0.439	0.317	0.080
ASCAT Index (-)	0	0.998	0.450	0.207
ASCAT CDF-matched with CDF1 (m^3m^{-3})	0.191	0.428	0.326	0.050
ASCAT CDF-matched with CDF2 (m^3m^{-3})	0.103	0.500	0.316	0.065
ASCAT CDF-matched with CDF2 seasonal (m^3m^{-3})	0.069	0.511	0.321	0.072
ASCAT CDF1 minus ECMWF (m^3m^{-3})	-0.11	0.198	0.010	0.054
ASCAT CDF2 minus ECMWF (m^3m^{-3})	-0.176	0.204	-0.001	0.056
ASCAT CDF2_seasonal minus ECMWF (m^3m^{-3})	-0.124	0.200	0.005	0.041

Table 05: Characteristics (minimum value, maximum value, mean and standard deviation) of ASCAT data and ECMWF SSM (H-TESSEL 36r4), and their difference for the improved ASCAT data rescaled with CDF1 and CDF2 without and with seasonal correction. Statistics were computed for a small region (12 pixels) in south west of France for the entire year 2009 (sample size after temporal collocation between ASCAT ECMWF SSM is 1972 elements).

Figure 11 illustrates, for one location in south west of France, an example of surface soil moisture time series obtained for 2009 for ECMWF (H-TESSEL cycle 36r4) and for ASCAT data, before (top panel) and after (middle panel) CDF matching. The middle panel shows that the current CDF matching (green) is not appropriate to be used with the current version of the land surface model at ECMWF as discussed above. Mean and variance of ASCAT data rescaled using CDF1 does not fit those of ECMWF land surface model. As expected using CDF2 (matching to H-TESSEL 36r4), improves the fit between rescaled ASCAT and ECMWF SSM compared to CDF1 (middle panel). However there are still large discrepancies related to the seasonal cycle differences between ASCAT and ECMWF soil moisture. Accounting for a seasonal correction (CDF2 seasonal, bottom panel) allows to obtain a much improved match, at short time scale at well as at seasonal and annual scales, between rescaled ASCAT data and ECMWF soil moisture (bottom panel).

Table 1 summarises, for a small region in south west of France (location above extended to 12 pixels), characteristics of ASCAT and ECMWF surface soil moisture and their difference (observation-model), for CDF1 and for CDF2 without and with seasonal correction. CDF1 rescales ASCAT to H-TESSEL version older than 36r4 (without the improved bare soil evaporation parameterisation and Leaf Area Index seasonal cycle). So, SSM range and SSM standard deviation (StD) is much lower when ASCAT is rescaled with CDF1 than with CDF2. Miminum soil moisture value of ASCAT data rescaled with CDF1 is 0.191 m^3m^{-3}, while it is 0.066 m^3m^{-3} for H-TESSEL cycle 36r4. Accordingly, the difference between ASCAT CDF1 and ECMWF shows a large positive bias of rescaled observations. Mean difference between observations and model drops from 0.01 m^3m^{-3} for CDF1 to -0.001 m^3m^{-3} for CDF2. Bias reduction between CDF1 and CDF2 shows the importance of using an updated version of the land surface model for the CDF matching. However the StD is not improved in CDF2 (0.056 m^3m^{-3}) compared to CDF1 (0.054 m^3m^{-3}). Accounting for the seasonal cycle correction is necessary to improve the fit between ASCAT and ECMWF SSM variance, as shown by reduced StD in observations minus model for CDF2 seasonal (0.041 m^3m^{-3}) compared to CDF2 (0.056 m^3m^{-3}). CDF2 seasonal also makes it possible to fit minimum soil moisture values to that of the model with a better accuracy than CDF2 (0.103 m^3m^{-3} for CDF2, 0.066 m^3m^{-3} for H-TESSEL and 0.069 m^3m^{-3}) for CDF2 seasonal).

4.3.4 Evaluation of the CDF matching for April 2011 data sets

Figures 12 and 13 show histograms of the global scale differences between ASCAT soil moisture after CDF matching and ECMWF operational soil moisture for the period 01 April 2011 to 21 April 2011, for the ASCAT operational product and the improved test product, respectively. Table 06 summarises statistics of the differences between observations and model for both the current and the improved ASCAT soil moisture products, for different configurations of CDF matching. Results show that: _

- The improved ASCAT soil moisture product is in better agreement with ECMWF soil moisture, than the operational ASCAT product, as shown in Table 06, with systematic lower mean and StD of the difference between observations and model, for all CDF matching approaches. For example for CDF2, StD is reduced from 0.08 m3m 3 for the operational product to 0.074 m^{3}m^{-3} for the improved product.
- Compared to CDF1, the improved matching CDF2 reduces the observations bias for both the operational ASCAT product (0.033 m^{3}m^{-3} for CDF1 and 0.014 m^{3}m^{-3} for CDF2) and the improved ASCAT product (0.034 m^{3}m^{-3} for CDF1 and 0.011 m^{3}m^{-3} for CDF2). Bias is slightly larger with the seasonal correction than without it. As for the regional case study above, accounting for seasonal correction in the CDF matching improves the match between observation and model variances, with StD values of 0.087 m^{3}m^{-3}, 0.074 m^{3}m^{-3} and 0.071 m^{3}m^{-3} for CDF1, CDF2 and CDF2 seasonal, respectively.

Both regional and global scale results confirm the suitability of the revised CDF matching approach. They show the relevance of both the seasonal bias correction and the improved ASCAT soil moisture product. Further investigations will be conducted when the improved ASCAT soil moisture is operational from 18 August 2011.

a) ASCAT CDF1 (used for SM-ASS-1)

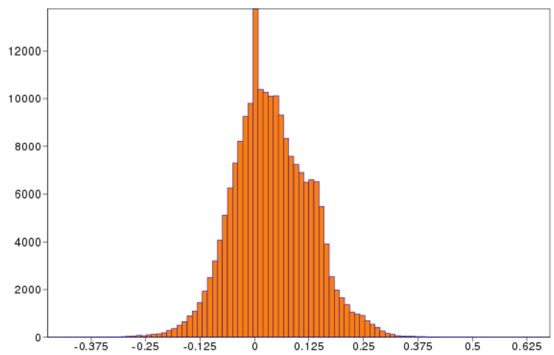

b) ASCAT CDF2

c) ASCAT CDF2 seasonal (used for SM-DAS-2)

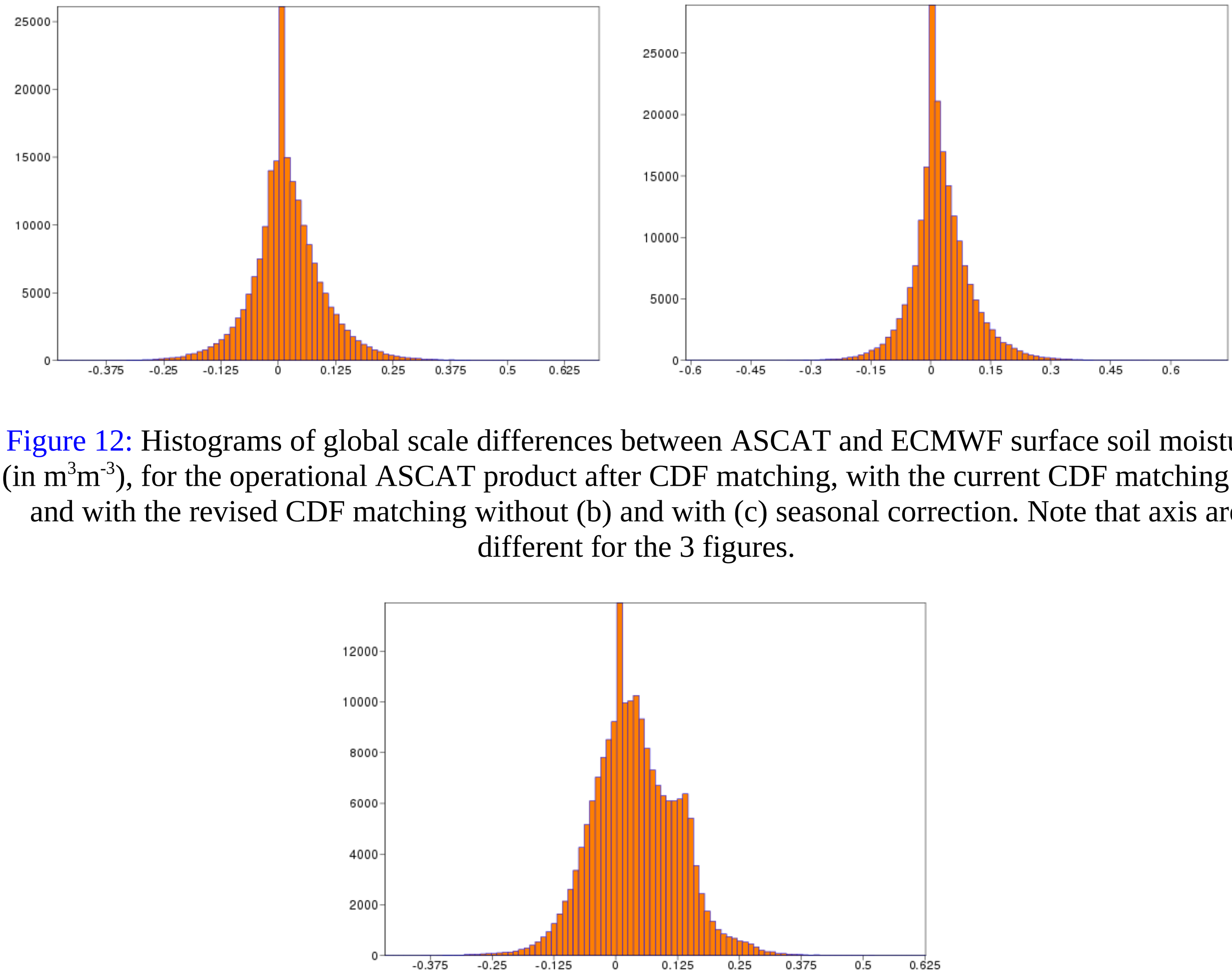

Figure 12: Histograms of global scale differences between ASCAT and ECMWF surface soil moisture (in m^3m^{-3}), for the operational ASCAT product after CDF matching, with the current CDF matching (a) and with the revised CDF matching without (b) and with (c) seasonal correction. Note that axis are different for the 3 figures.

a) ASCAT CDF2 c) ASCAT CDF2 seasonal (used for SM-DAS-2)

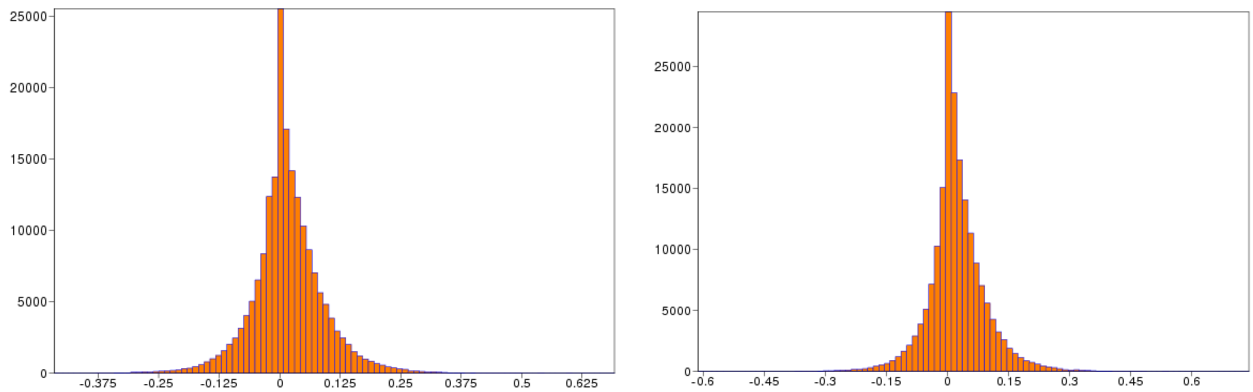

Figure 13: Same as Figure 12 but for the new ASCAT surface soil moisture product (as released since 18 August 2011 by EUMETSAT).

	Old ASCAT SSM product		New ASCAT SSM product	
	Mean	StD	Mean	StD
CDF1	0.033	0.090	0.034	0.087

CDF2	0.014	0.080	0.011	0.074
CDF2 seasonal	0.020	0.074	0.017	0.071

Table 06: Global scale statistics of the difference (in m3m 3) between ASCAT observations after CDF matching and ECMWF operational soil moisture, for 01-21 April 2011, for different configurations of ASCAT bias correction. Sample size after ASCAT and H-TESSEL quality control and CDF matching is 200228.

4.3.5 Analysis Experiments and Monitoring

A set of analysis experiments was conducted to evaluate (i) the suitability of the improved product (released by EUMETSAT from 18 August 2011) for the operational ASCAT monitoring at ECMWF, (ii) the impact of the improved product on the soil moisture analysis for the SM-DAS-2 production chain. Table 07 summarises the experiments, using either the old ASCAT product or the improved product, with CDF1 and CDF2 seasonal.

	ASCAT old product	ASCAT new product
CDF1	fk03	fk6n
CDF2 seasonal	fk04	fk8o

Table 07: Analysis experiments name conducted with the old ASCAT product (EUMETSAT product before 18 August 2011) and new ASCAT product (as released by EUMETSAT since 18 August 2011) and using the old CDF matching (used for SM-ASS-1) and the new CDF matching CDF2 with seasonal correction (used for SM-DAS-2).

Different ASCAT SSM CDF matching were used and compared in experiments with activated ASCAT SSM data assimilation (fk03, fk04, fk6n and fk6o). All the experiments were conducted for 27 March 2011 to 21 April 2011 using the up to date surface analysis as used in IFS cycle 37r2. This period was chosen because EUMETSAT provided a test ASCAT soil moisture data set using the new retrieval algorithm.

Figure 14 presents ASCAT soil moisture monitoring, for the 4 experiments fk03 (ASCAT old, CDF1), fk6n (ASCAT old, CDF2 seasonally corrected), fk04 (ASCAT new, CDF1) and fk6o (ASCAT new, CDF2 seasonally corrected). It clearly shows an improved usage of the ASCAT data when the new improved product is used (bottom) compared to the old operational ASCAT product (top). The angular dependency of the first guess departure for the old operational product (black line, top panel) is removed with the new product (black line, bottom panel). Colour scale indicates that more data is used (i) with the improved product (bottom) than with the operational product (top) (ii) with the revised CDF matching (right) than with CDF1 (left). This confirms again the relevance of both the improved ASCAT product and the revised CDF matching used for the SM-DAS-2 production chain.

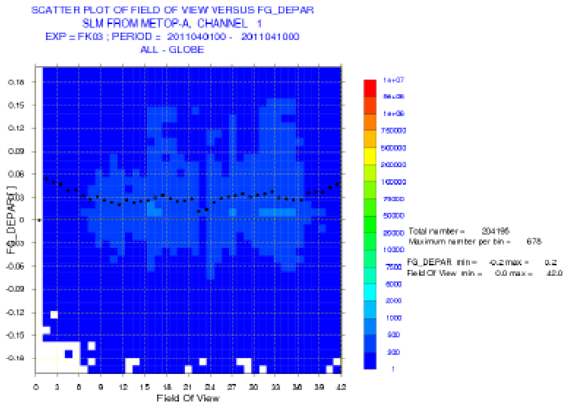

(a) ASCAT Operational Product: CDF1 (fk03, left) CDF2 seasonal (fk6n, right)

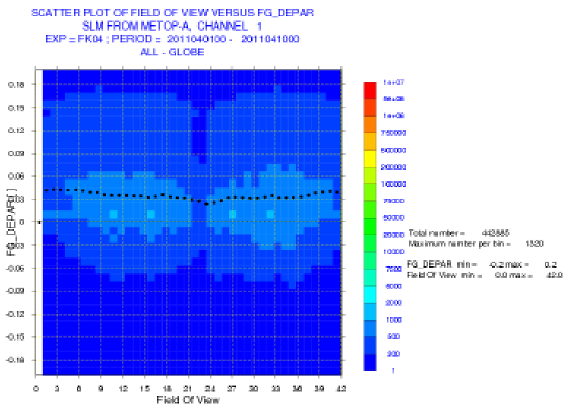

(b) ASCAT Improved Product: CDF1 (fk04, left) CDF2 seasonal (fk6o, right)

Figure 14: ASCAT SSM first guess departure (difference between rescaled observation and model first guess, dotted black line), as a function of the ASCAT incidence angle (Field of View on x-axis, ie ASCAT node), for four experiments using the operational (top) and improved (bottom) ASCAT products with the old matching CDF1 (left) and revised matching CDF2 seasonal (right) . Colour scale indicates the number of data used after CDF matching as a function of first guess departure range and Field of View.

To summarise a revised ASCAT soil moisture CDF matching approach was developed for SM-DAS-2. ASCAT CDF matching results are shown, at the point scale, at regional scale and at global scale, for the ASCAT operational product and the ASCAT improved product. Compared to the original CDF matching, the revised CDF matching reduces the observations bias for both the operational ASCAT product and the improved ASCAT product. Accounting for a seasonal correction in the revised CDF matching improves further the match of ASCAT to ECMWF SSM,at short time scale at well as at seasonal and annual scales. At global scale results combining the seasonally corrected bias correction and the improved ASCAT product gave the best agreement in terms of StD between rescaled ASCAT soil moisture and ECMWF operational soil moisture. Data assimilation experiments were conducted to address the impact of improved ASCAT data assimilation and revised ASCAT SSM CDF matching for monitoring and assimilation of ASCAT SSM.

Operational monitoring of the EUMETSAT-CAF ASCAT surface soil moisture product is peformed Near Real Time at ECMWF since 8 September 2009:
http://www.ecmwf.int/products/forecasts/d/charts/monitoring/satellite/slmoist/ASCAT/

The ASCAT surface soil moisture monitoring represents, in Near Real Time, different features and statistics of the EUMETSAT-CAF ASCAT surface soil moisture product (converted in volumetric soil moisture). Monitoring includes time-averaged geographical mean fields, time series of area averages, Hovmoeller diagrams, scatter plots, for both observation and first guess departure (EUMETSAT CAF soil moisture product minus ECMWF soil moisture). Monitoring results conducted with the current pre-operational ECMWF IFS cycle (esuite 37r3, already running in parallel to the operational cycle) confirm the relevance of combining the improved ASCAT product and the revised CDF matching, as shown in Fig. 15. The current ECMWF esuite 37r3 will become operational in November 2011. So, in revised CDF matching will be used routinely from IFS cycle 37r3 for ASCAT CAF operational monitoring at |ECMWF.

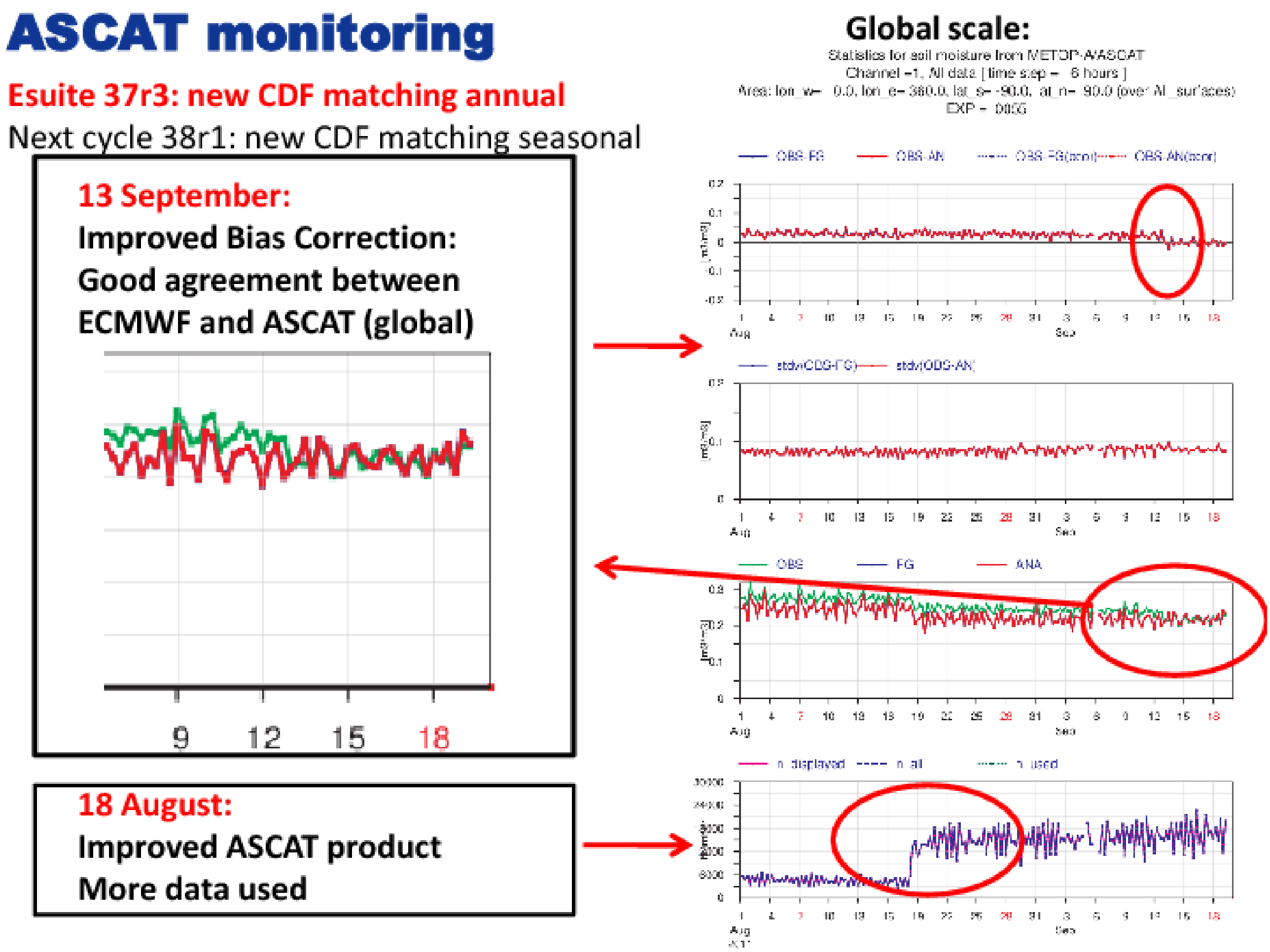

Figure 15: ASCAT CAF product operational monitoring (observation CDF matched and difference with ECMWF soil moisture) in the experimental suite (esuite) 37r3 that will come into operations in November 2011. The NEW ASCAT CAF product was delivered from 18 August 2011. The SM-DAS-2 CDF matching was implemented in the esuite on 13 September 2011. They both contribute to improve the efficiency of ASCAT data assimilation in the land surface analysis system.

4.4 ECMWF simplified Extended Kalman filter

A number of current operational soil moisture analysis systems in Numerical Weather Prediction (NWP) are based on analysed or observed screen-level variables, (2 m temperature and relative humidity). At Météo France (Giard and Bazile, 2000), ECMWF (Mahfouf et al., 2000) and at Environment Canada (Bélair et al., 2003) as well as in the High Resolution Limited Area Model (HIRLAM, Rodriguez et al., 2003) Optimal Interpolation (OI) algorithm is used operationally. The OI scheme presents several weaknesses, including the fact that it is not flexible enough to cope with the current increase in model complexity and data availability. Land surface processes and their initialisation are of crucial importance to address the challenge of seamless (from weather to seasonal) NWP. In particular it is expected to be of high interest to assimilate new satellite based soil moisture observations from ASCAT or SMOS.

The German Weather Service (Deutsche Wetter Dienst) was the first NWP centre to adopte a simplified Extended Kalman Filter (SEKF) (Hess, 2001). Météo-France developed an offline SEKF soil analysis scheme within the SURFace EXternalized system used for research applications (Mahfouf et al., 2008, Mahfouf, 2010). ECMWF also recently developed an SEKF system for the soil moisture analysis. First investigations were conducted at locale scale (Seuffert et al., 2003), and at global scale by Drusch et al. (2009) who describe the SEKF surface analysis and show preliminary one-day results at coarse resolution (125 km). In contrast the UK Metoffice uses a simple analytical approach to analyse soil moisture. They assimilate ASCAT soil moisture together in operations using this nudging approach (Dharssi et al., 2011). The advantage was to enable a fast implementation of the use of ASCAT data. However on the longer term this system is not flexible to develop multi-variate data assimilation system and it does not allow to combine ASCAT data with other type of data (e.g. SMOS).

Based on developments conducted at ECMWF, the new soil moisture analysis scheme based on a point-wise simplified Extended Kalman Filter (EKF) was implemented at ECMWF with cycle 36r4 of the Integrated Forecasting System (IFS) in November 2010 (de Rosnay et al., 2011a). The EKF soil moisture analysis replaces the previous Optimum Interpolation (OI) scheme, which was used in operations from July 1999 (Mahfouf, 2000) to November 2010. In continuity with the previous system it uses 2-metre air temperature and relative humidity observations to analyse soil moisture. The computing cost of the EKF soil moisture analysis is significantly higher than that of the OI scheme. So, as part of the EKF soil moisture analysis implementation, a new surface analysis structure was implemented in September 2009 (cycle 35r3) to move the surface analysis out of the time critical path.

The main justifications for implementing the EKF soil moisture analysis are as follows.

- In contrast to the OI scheme, which uses fixed calibrated coefficients to describe the relationship between an observation and model soil moisture, the EKF soil moisture increments result from

dynamical estimates that quantify accurately the physical relationship between an observation and soil moisture.
- The EKF scheme is flexible to cope with the current increase in model complexity. In particular, changes in the IFS and in the land-surface model H-TESSEL (Hydrology Tiled ECMWF Scheme for Surface Exchanges over Land) are accounted for in the analysis increments computation.
- The EKF soil moisture analysis makes it possible to use soil moisture data from satellites and to combine different sources of information (i.e. active and passive microwave satellite data, and conventional observations).
- It considers the observation and model errors during the analysis in a statistically optimal way and allows assimilation of observations at their correct observation times.

The EKF coefficients are dynamically estimated, so the soil moisture corrections account for meteorological forcing (radiative and precipitation) and soil moisture conditions. There is also the possibility of simultaneously assimilating screen-level observations and satellite data such as ASCAT surface soil moisture, as it is done for the SM-DAS-2 production chain or SMOS brightness temperature products (under investigation for an other project between ESA and ECMWF). The EKF soil moisture analysis is a point wise data assimilation scheme. For each grid point, the analysed soil moisture state vector $\boldsymbol{\theta}_a$ is computed as:

$$\boldsymbol{\theta}_a = \boldsymbol{\theta}_b + \boldsymbol{K}\,(\boldsymbol{y} - \mathcal{H}\,\boldsymbol{\theta}_b)$$

with $\boldsymbol{\theta}_b$ the background soil moisture state vector, $\boldsymbol{H}$ the non-linear observation operator, $\boldsymbol{y}$ the observation vector and $\boldsymbol{K}$ the Kalman gain matrix which accounts for the Jacobian matrix $\mathbf{H}$ of the observation operator, and the covariance matrix of background and observation errors. The EKF implemented at ECMWF uses a static covariance matrix of background errors, which is diagonal (using estimated background error variance). This simplified EKF is identical to a simplified 2D-Var. For SM-DAS-2 data assimilation chain, the soil moisture background error standard deviation is 0.01 m3.m-3 and ASCAT observation error standard deviation is twice the model error, so that a larger confidence level is given to the model. This error specification is currently under revision to account for recent ASCAT validation results and frist-guess departure statistics and it will be updated by the end of the H-SAF CDOP. In the SM-DAS-2 production chain the observation vector includes:

- Conventional observations: 2-metre temperature and relative humidity.
- ASCAT CAF Surface Soil Moisture measurements

The elements of the Jacobian matrix used in the analysis scheme are estimated in finite differences by perturbing individually each analysed soil layer. In contrast to the OI scheme, the EKF Jacobians are computed for each soil layer to account for the soil water diffucion processes. Therefore computed soil moisture increments for each grid point of the model follow a vertical profile that results from a physically-based estimate of the relationship between the soil moisture profile and the parameters in the lower atmospheric level.

The EKF is a dynamical scheme that accounts for non-linear control on the soil moisture increments (meteorological forcing and soil moisture conditions). It is described in de Rosnay et al. (2011a) and in Drusch et al., (2009) as well as in Seuffert et al, (2004) So, it prevents undesirable and excessive soil moisture corrections, and reduces the soil moisture analysis increments. This significantly improves the performance of the soil moisture analysis, as verified against independent soil moisture observations.

The new analysis scheme has a moderate impact on the atmospheric scores although it slightly improves the 2-metre temperature by reducing the cold bias in Europe and Africa.

The EKF soil moisture analysis enables the combined use of screen-level parameters and satellite data, such as ASCAT soil moisture data, to analyse soil moisture. Results with ASCAT data assimilation show a neutral impact on both soil moisture and screen-level parameters when compared to results of data assimilation experiments without ASCAT data assimilation (de Rosnay et al., 2011a). However very recent improvements in the ASCAT soil moisture products and in bias correction clearly improve the ASCAT ASCAT soil moisture data usage in the SM-DAS-2 data assimilation chain, as shown in OSSE described in de Rosnay 2011a,b.

(6)

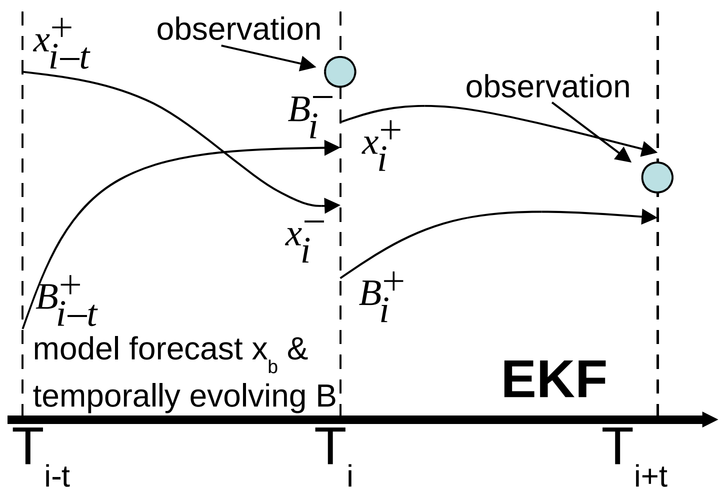

Fig. 13 - Schematic outline of the extended Kalman filter.

4.5 ECMWF Early delivery suite

The EKF as described in the previous section is implemented in the Integrated Forecast System. ***Fig. 14*** shows the current operational schedule as introduced in 2004. A comprehensive description of the operational system is given in Haseler 2004; this section gives a short summary of the most relevant parts. The atmospheric 12-hour 4D-Var analyses use observations from 21:01 UTC to 09:00 UTC and 09:01 UTC to 21:00 UTC. These analyses are run with a delayed-cut-off time, in order to use the maximum possible number of observations. The extraction tasks for observations in the periods 21:01 - 03:00 UTC and 03:01-09:00 UTC are run at 13:45 and 14:00 UTC respectively, while the extraction tasks for observations in the periods 09:01 - 15:00 UTC and 15:01-21:00 UTC are run at 01:45 and 02:00 UTC, respectively.

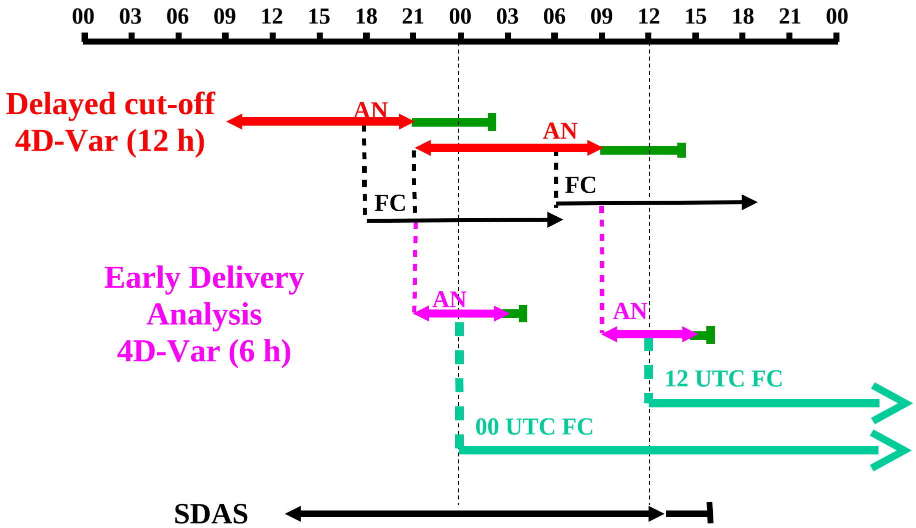

Fig. 14 - The IFS early delivery configuration, implemented in September 2004 (Haseler 2004).

The early-delivery analyses have been introduced to make the ECMWF operational products available earlier. In particular, it makes the 00:00 UTC products available before the end of the working day, even in the easternmost Member States where local summer time is three hours ahead of Universal Time. These analyses do not propagate information from cycle to cycle. Each analysis is reinitialized with the best available model fields from the delayed-cut-off assimilation. The 00:00 UTC early-delivery analysis is a 6-hour 4D-Var analysis that uses observations in the window 21:01-03:00 UTC. The cut-off time is 04:00 UTC, and any observations that arrive after this time are not used by the early-delivery analysis. The first guess for the 00:00 UTC early-delivery analysis is the nine-hour forecast from the previous day's 12 UTC delayed-cut-off 12-hour 4D-Var analysis. The 12:00 UTC early-delivery analysis is a 6-hour 4D-Var analysis that uses observations in the window 09:01-15:00 UTC. The cut-off time is 16:00 UTC. The first guess for the 12:00 UTC early-delivery analysis is the nine-hour forecast from the 00:00 UTC delayed-cut-off 12-hour 4D-Var analysis. Ten-day forecasts are run from the early-delivery analyses at 00 and 12 UTC.

The analyses for the screen-level variables (i.e. 2 m temperature and relative humidity) and snow water equivalent are based on synoptic observations for 00:00, 06:00, 12:00, and 18:00 UTC. The corresponding model first guess are six- and 12-hourly forecasts from 18:00 UTC and 06:00 UTC, respectively. These short-range forecasts are initialized with analyses from the delayed-cut-off cycle. Since the screen-level analyses rely on the delayed-cut-off analyses, 00:00 and 06:00 UTC analyses are available at around 15:30 UTC. The analyses for 12:00 and 18:00 UTC are ready at 03:30 UTC. Consequently, the operational 10-day forecasts have to rely on nine-hour forecast screen-level variables as well.

The EKF surface analysis uses a 12-hour data assimilation window which runs in parallel to the 4D-Var atmospheric data assimilation system. In order to be available in time for the 10-day forecasts, the soil moisture analyses are finished by 16:00 or 04:00 UTC.

5 Validation activities of SM-DAS-2 product

The SEKF soil moisture analysis is shown in de Rosnay et al. (2011a) to drastically reduce the soil moisture analysis increments. Using the SEKF soil moisture analysis generally improves the 2 meter temperature scores, by reducing the cold bias. Specific humidity shows generally dryer conditions with the SEKF than with the OI. Soil moisture evaluation against ground measurements from the SMOSMANIA network is also presented (layers 1 and 2). ECMWF soil moisture is in general good agreement with ground observations, with correlations values higher than 0.78 for the two layers. Using the SEKF instead of the OI improves significantly the soil moisture analysis, leading to noteworthy agreement between ECMWF soil moisture and ground truth (mean correlation higher than 0.84 for SEKF against the SMOSMANIA data). SM-DAS-2 is a high quality products as already anticipated with its precursor product, the volumetric root zone product SM-ASS-1 during the H-SAF development phase (Albergel et al., 2010, Brocca et al., 2010).

This section reports on the validation results of the retrieved root zone soil moisture profile index SM-DAS-2. SM-DAS-2 is evaluated against more than 200 in situ stations located in Africa, Australia, Europe and United States are to determine its reliability to represent the soil moisture annual cycle as well as its short term variability. Along with SM-DAS-2, we found relevant to present an evaluation of two remotely sensed soil moisture products, namely ASCAT (Advanced scatterometers used in SM-DAS-2 production) and SMOS (Soil Moisture Ocean Salinity). Evaluation of the times series as well as of the anomaly values, show good performances of the three products to capture surface soil moisture annual cycle and short term variability. Correlations with in situ data are very satisfactory over most of the investigated sites located in contrasted biomes and climate conditions with averaged values of 0.70 for SM-DAS-2, 0.53 for ASCAT and 0.54 for SMOS. Although radio frequency interference disturbs the natural microwave emission of Earth observed by SMOS in several parts of the world, hence the soil moisture retrieval, performances of SMOS over Australia are very encouraging.

In situ soil moisture observations are necessary to evaluate both remotely sensed and modelled soil moisture. In the recent years huge efforts were made to make available such observations in contrasting biomes and climate conditions. Some of them are now freely available on the Internet. The different soil moisture data sets used in this study are presented in Figure 15. For each station available, a quality check of the data was performed and suspicious data were eliminated. 229 of 252 available stations were retained for this study, so 23 of them were rejected from this first visual quality check.

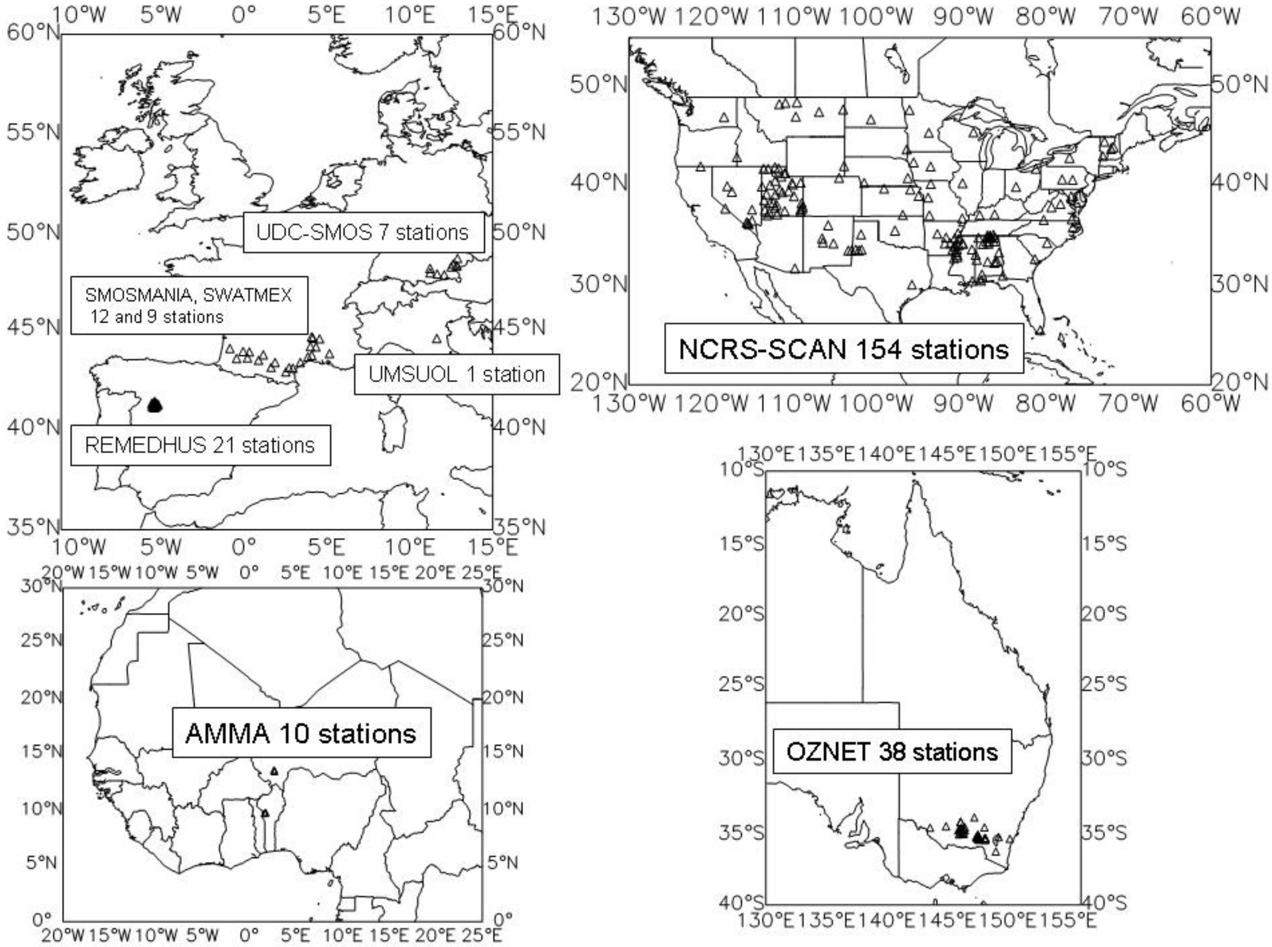

Figure 15: Location of the different in situ soil moisture stations used in this study, 38 in Australia (OZNET network), 154 within the United States (NCRS-SCAN network), 10 in Western Africa (AMMA network), 21 in southwestern France (SMOSMANIA and SWATMEX networks), 7 in Germany (UDC-SMOS network) and 1 in Italy (UMSUOL).

ASCAT SSM estimates represent a relative measure of the soil moisture in the first centimetres of soil and it is given in percent, SM-DAS-2 is an index (between [0,1]), SMOS and in situ data are in m^3m^{-3}. Hence, to enable a fair product comparison, all soil moisture data sets (in situ, remotely sensed and modelled) are scaled between [0,1] using their own maximum and minimum values over the year 2010. The nearest neighbour technique is used to make a correspondence between SM-DAS-2, ASCAT, SMOS and in situ SSM. Time steps for in situ data range from 12-min (e.g. SMOSMANIA, SWATMEX) to 1 hour (e.g. NCRS-SCAN). SM-DAS-2, ASCAT, SMOS and in situ SSM are available at different time of the day, each of them is collocated in time with ground observations.

For all stations, correlations (R), bias (in situ minus analysis), root mean square difference (RMSD) are calculated for the whole 2010 year. Additionally, the p-value (a measure of the correlation significance), it indicates the significance of the test, the 95% confidence interval is used in this study configurations where the p-value is below 0.05 (i.e. the correlation is not a coincidence) are retained. In situ data contain errors (instrumental and representativeness), so they are not considered as 'true' soil moisture. This is underlined here by using the RMS Difference terminology instead of RMS Error.

Additionally, the normalised standard deviation (SDV) and the centred root mean square difference between analysis and in situ patterns, normalised by the in situ standard deviations (E) are computed.

SDV is the ratio between SSM product and in situ standards deviations; it gives the relative amplitude whilst E quantifies errors in the pattern variations. It does not include any information on biases since means of the fields are subtracted before computing second order errors. SDV and E are expressed by Eq.2 and Eq.3, respectively:

$$SDV = \sigma_{SSM_{product}} / \sigma_{SSM_{insitu}} \qquad \text{Eq.2}$$

$$E^2 = \left(RMSD^2 - Bias^2\right) / \sigma^2_{insitu} \qquad \text{Eq.3}$$

R, SDV and E are complementary but not independent as they are related by Eq.4 (Taylor, 2001):

$$E^2 = SDV^2 + 1 - 2 \cdot SDV \cdot R \qquad \text{Eq.4}$$

Taylor diagrams are used to represent these three different statistics on two dimensional plots. The normalized standard deviation is displayed as a radial distance and the correlation with in situ data as an angle in the polar plot. In situ data are represented by a point located on the x axis at R=1 and SDV=1. The distance to this point represents the centred normalized RMS difference (E) between the analysis and in situ patterns.

The statistical scores for the comparison between SM-DAS-2, ASCAT, SMOS (referred as ECM, ASC and SMO in the following of the paper) and in situ SSM are presented in Table 8. Only the configurations associated to significant correlation values (p-value < 0.05) are considered leading to 219, 208 and 180 stations available for ECM, ASC and SMO, respectively. In average, for all the stations, correlation values are 0.70, 0.53 and 0.54 for ECM, ASC and SMO. SMOSMANIA in southwestern France and OZNET in Australia present the best correlation values for ECM (0.83 and 0.82 in average) while AMMA in western Africa presents a correlation value average of 0.45.

Table 8: Comparisons of normalised SSM between in situ observations and products; SM-DAS-2 (ECM), ASCAT (ASC) and SMOS (SMO) for 2010. Mean correlation, bias (in situ minus products) and root mean square difference (RMSD) are given for each network and for each product. Scores are presented for significant correlations with p-values < 0.05.

Soil Moisture data set	Number of stations with p-values<0.05			Correlation [-]			Bias [-]			RMSD [-]		
	ECM	ASC	SMO	ECM	ASC	SMO	ECM	ASC	SMO	ECM	ASC	SMO
SMOSMANIA (France)	11	11	10	0.83	0.52	0.44	-0.178	-0.037	0.124	0.242	0.254	0.273
SWATMEX (France)	9	8	6	0.79	0.33	0.40	-0.274	-0.140	0.101	0.345	0.284	0.235
OZNET (Australia)	36	34	30	0.82	0.80	0.74	-0.013	-0.021	0.195	0.178	0.184	0.255
NCRS-SCAN (US)	131	125	106	0.65	0.48	0.51	-0.022	-0.078	0.095	0.233	0.266	0.232
AMMA (West Africa)	5	6	6	0.45	0.55	0.42	-0.074	-0.179	0.079	0.531	0.407	0.316
REMEDHUS (Spain)	17	17	17	0.79	0.57	0.52	-0.118	-0.088	0.128	0.243	0.245	0.232
UMSUOL (Italy)	1	1	1	0.76	0.39	0.54	-0.176	0.077	0.167	0.233	0.237	0.240
UDC-SMOS (Germany)	9	6	4	0.59	0.30	0.29	-0.061	0.052	0.267	0.198	0.267	0.344
All stations	219	208	180	0.70	0.53	0.54	-0.050	-0.068	0.120	0.235	0.255	0.243

Biases are in average of -0.050, -0.068 and 0.120 (in situ minus SSM products, dimensionless) for ECM, ASC and SMO, respectively. Negative biases are found with ECM, it concerns all networks used in this study. On the contrary, SMO systematically presents positive averaged biases. Averaged RMSD are 0.235, 0.255 and 0.243 for ECM, ASC and SMO, respectively. The RMSD represents the relative error of the soil moisture dynamical range. The average dynamic range observed for each network, associated to the average RMSD values of each network permits to give an estimate of the average error in volumetric soil moisture; about 0.07 m^3m^{-3}, 0.08 m^3m^{-3} and 0.08 m^3m^{-3} for ECM, ASC and SMO, respectively.

Figure 16 presents three Taylor diagrams illustrating the statistics of the comparison between ECM, ASC and SMO and in situ data. They correspond to three networks used in this study, REMEDHUS in Spain, OZNET in Australia and SMOSMANIA in France. These diagrams underline the good range of correlation obtained for ECM with most of the values between 0.70 and 0.90 while ASC and SMO present lower values. It is particularly clear for SMOSMANIA (Fig. 16C), moreover, for this network, symbols representing ASC and SMO are most of the time below the SDV value of 1 (red dashed line on Figure 16); as SDV is the ratio between analysed and in situ standard deviation (see Eq.2) it indicates that the variability of the in situ data is higher than the one of ASC and SMO for this group of stations. For the OZNET network (Fig. 16B) however, the three products present good levels of correlation (most of the time above 0.70).

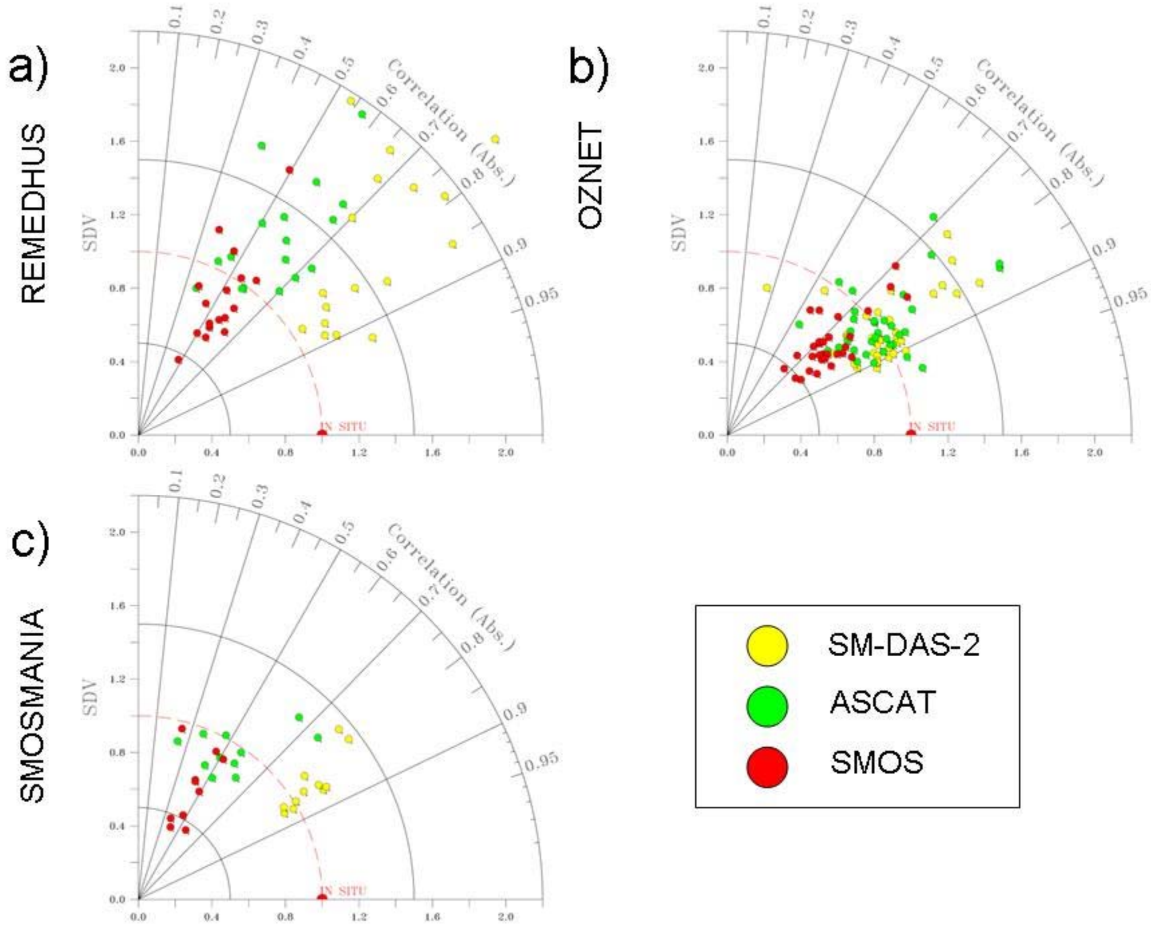

Figure 5: Taylor diagram illustrating the statistics of the comparison between SM-DAS-2, ASCAT, SMOS and in situ SSM for a) the REMEDHUS network in Spain, b) the OZNET network in Australia and c) the SMOSMANIA network in France. Yellow circles are for SM-DAS-2, green circles for ASCAT and red circles for SMOS.

More information can be found in the Visiting Scientist mid-term report "Comparison between H-SAF large scale surface soil moisture, H-SAF assimilated soil moisture and SMOS level 2 soil moisture" (VS-11 02) as well as is the Product Validation Report of SM-DAS-2.

6 References

Albergel, C., R¨udiger, C., Pellarin, T., Calvet, J.-C., Fritz, N., Froissard, F., Suquia, D., Petitpa, A., Piguet, B., and Martin, E.: From near-surface to root-zone soil moisture using an exponential filter: an assessment of the method based on in-situ observations and model simulations, Hydrol. Earth Syst. Sci., 12, 1323–1337, doi:10.5194/hess-12-1323-2008, 2008.

Albergel, C., J.-C. Calvet, P. de Rosnay, G. Balsamo, W. Wagner, S. Hasenauer, V. Naeimi, E. Martin, E. Bazile, F. Bouyssel, J.-F. Mahfouf, "Cross-evaluation of modelled and remotely sensed surface soil moisture with in situ data in southwestern France", Hydrol. and Earth Syst. Sci., 14, 2177-2191, doi:10.5194/hess-14-2177-2010, 2010

Albergel, C., P de Rosnay, G. Balsamo, L. Isaksen,J. Muñoz Sabater, 2011: Soil moisture analysis at ECMWF: evaluation using global ground-based in situ observations, submitted to J. of Hydrometeorology, 2011

Albergel C., P. de Rosnay, C. Gruhier, J. Muñoz Sabater, S. Hasenauer, L. Isaksen, Y. Kerr and W. Wagner: Evaluation of remotely sensed and modelled soil moisture products using global ground-based in-situ observations, submitted to Remote Sensing of Environment, 2011

Bélair, S., L.-P. Crevier, J. Mailhot, B. Bilodeau, and Y. Delage, 2003: Operational implementation of the ISBA land surface scheme in the Canadian regional weather forecast model. Part I: Warm season results. J. Hydromet., 4,

Balsamo G., P. Viterbo, A. Beljaars, B. Van den Hurk, A.K. Betts and K. Scipal, 2009: "A revised hydrology for the ECMWF model: Verification from field site to terrestrial water storage and impact in the Integrated Forecast System". *J. Hydrometeorol.*, 10, 623-643.

G. Balsamo, S. Boussetta, E. Dutra, A. Beljaars, P. Viterbo, B. Van den Hurk, 2011: Evolution of land surface processes in the IFS, ECMWF Newsletter, 127, 17-22.

Balsamo, G., S. Boussetta, P. Lopez, L. Ferranti, 2010: Evaluation of ERA-Interim and ERA-Interim-GPCPrescaled precipitation over the U.S.A., ERA Report Series, n. 5, pp10

Bartalis Z., Hasenauer, S., Naeimi V. and Wagner W., Institute of Photogrammetry and Remote Sensing, Vienna University of Technology, Austria, WRAP-NRT 2.0 Refernce Manual, ACSTA soil moisture report series, No 14, 2007

S. Boussetta, G. Balsamo, A. Beljaars, T. Kral, L. Jarlan, 2011: Impact of a satellite-derived Leaf Area Index monthly climatology in a global Numerical Weather Prediction model, Int. J. Remote Sensing (in press)

Brocca, L. S. Hasenauer, P. de Rosnay et al.: Consistent validation of H-SAF soil moisture satellite and model products against ground measurements for selected sites in Europe H-SAF Development Phase VS SM_0903 (http://hsaf.meteoam.it/documents/reference/HSAF_AS_09_03_final_report.pdf)

Cosby B., G. Hornberger, R. Clapp and T. Ginn, 1984: "A statistical exploration of the relationship of soil moisture characteristics to the physical properties of soils". *Water Res. Res.*, **20**, 682-690.

de Rosnay P. 2009: "Sensitivity of ASCAT soil moisture first guess departure to incidence angle". *ECMWF Research department memorandum 0953,* July 2009.

de Rosnay P., M. Drusch, G. Balsamo, C. Albergel, L. Isaksen, 2011: "Extended kalman Filter Soil-Moisture analaysis in the IFS". ECMWF Newsletter, 127, 12-16. 2011 a

de Rosnay P, G. De Chiara, I. Mallas: Use of ASCAT soil moisture: revised bias correction and test of improved ASCAT product in IFS cycle 37r2, R43.8/PdR/11100, 2011 b

de Rosnay P: Use of ASCAT Level 2 Multi-parameter BUFR Product in operations in IFS cycle 36r4, R58.3/PdR/1128, 2011 c

Dharssi, I., Bovis, K., Macpherson, B., and Jones, C.: Operational assimilation of ASCAT surface soil wetness at the Met Office, Hydrol. Earth Syst. Sci. Discuss., 8, 4313-4354, doi:10.5194/hessd-8-4313-2011, 2011.

Draper, C. S., J.-F. Mahfouf and J.P. Walker, 2009: An EKF assimilation of AMSR-E soil moisture into the ISBA land surface scheme, J. Geophys. Res., VOL. 114, D20104, doi:10.1029/2008JD011650, 2009

De Vries D.A., 1975: "Heat transfer in soils". In '*Heat and mass transfer in the biosphere. Part I: Transfer processes in the plant environment*". D.A. DeVries and N.H. Afgan, Editors, Wiley, 4-28.

Dee D. and A. da Silva, 1998: "Data assimilation in the presence of forecast bias". *QJR Met. Soc.*, **124**, 269-295.

Drusch M., E.F. Wood and H. Gao, 2005: "Observation operators for the direct assimilation of TRMM microwave imager retrieved soil moisture". *Geo. Res. Let*., **32**, L15403, doi:10.1029/2005GL023623.

Drusch M., K. Scipal, P. de Rosnay, G. Balsamo, E. Andersson, P. Bougeault and P. Viterbo, 2009: "Towards a Kalman Filter based soil moisture analysis system for the operational ECMWF Integrated Forecast System, Geophys." *Res. Lett.,* 36, L10401, doi:10.1029/2009GL037716.

ECMWF, 2008: "Integrated Forecast System Documentation". *[available online at http://www.ecmwf.int/research/ifsdocs/]*.

FAO, 2003: "Digital soil map of the world (DSMW)". *Technical report*, Food and Agriculture Organization of the United Nations, re-issued version.

Gelb A., Ed.1974: "*Applied Optimal Estimation*". The MIT Press, 374 pp.

Hahn, S. & Wagner, W. (2011). Characterisation of calibration-related errors on the initial METOP ASCAT soil moisture product, *Geophysical Research Abstract*, 13, EGU2011-3178.

Haseler, 2004: "Early delivery suite". Technical Memorandum 454, 45 pp *[available through ECMWF, Reading, UK]*.

Hess R., 2001: "Assimilation of screen-level observations by variational soil moisture analysis". *Met. Atmos. Phys.*, **77**, 145-154.

Koster R.D. and P.C.D. Milly, 1997: "The interplay between transpiration and runoff formulations in land surface schemes used with atmospheric models". *J. Climate*, **10**, 1578-1591.

Mahfouf, **J.-F.**, 2000: A revised land-surface analysis scheme in the Intergrated Forecasting System. *ECMWF Newsletter No. 88*, 8–13,

Mahfouf, J., K. Bergaoui, C. Draper, F. Bouyseel, F. Taillefer, and L. Taseva, 2008: A comparison ot two off-line soil analysis schemes for assimilation of screen level observations. J. Geophys. Res., 114, D08105, doi:10.1029/2008JD011077 2009.

Mahfouf, J.-F. (2010), Assimilation of satellite-derived soil moisture from ASCAT in a limited-area NWP model. Quarterly Journal of the Royal Meteorological Society, 136: 784\u2013798. doi: 10.1002/qj.602

Naeimi V., K. Scipal, Z. Bartalis, S. Hasenauer and W. Wagner, 2009: An improved soil moisture retrieval algorithm for ERS and METOP scatterometer observations, *IEEE Trans. Geosc. Remote Sens.*, vol.47, pp.1999-2013.

Patterson K., 1990: "Global distribution of total and total-available soil water holding capacities". MS-Thesis, Department of Geography, University of Delaware.

Peters-Lidard C., E. Blackburn, X. Liang and E.F. Wood, 1998: "The effect of soil conductivity parameterization on surface energy fluxes and temperature". *J. Atm. Sci.*, **55**, 1209-1224.

Reichle R. and R.D. Koster, 2004: "Bias reduction in short records of satellite soil moisture". *Geo. Res. Let.*, **31**, L19501, doi:10.1029/2004GL020938.

Reichle R., D.B. McLaughlin and D. Entekhabi, 2002: "Hydrologic data assimilation with the Ensemble Kalman Filter". *Mon. Wea. Rev.*, **130**, 103-114.

Scipal K., M. Drusch and W. Wagner, 2008a: "Assimilation of a ERS scatterometer derived soil moisture index in the ECMWF numerical weather prediction system". Advances in water resources, doi:10.1016/j.advwatres.2008.04013.

Scipal K., T. Holmes, R. de Jeu, V. Naeimi and W. Wagner 2008b: "A possible solution for the problem of estimating the error structure of global soil moisture data sets". *Geophys. Res. Lett.*, 35, L24403, doi:10.1029/2008GL035599.

Seuffert G., H. Wilker, P. Viterbo, J.F. Mahfouf, M. Drusch and J.C. Calvet, 2003: "Soil moisture analysis combining screen-level parameters and microwave brightness temperature: A test with field data". *Geophys. Res. Lett.*, **30 (10)**, 10.1029/2003GL017144.

Seuffert G., H. Wilker, P. Viterbo, M. Drusch and J.F. Mahfouf, 2004: "On the usage of screen level parameters and microwave brightness temperature for soil moisture analysis". *J. Hydromet*., **5**, 516-531.

U.S. Geological Survey, 1999: "Global Land Cover Characterization". *[available online under http://edcsns17.cr.usgs.gov/glcc/]*.

Van den Hurk B., P. Viterbo, A. Beljaars and A. Betts, 2000: "Offline validation of the ERA40 surface scheme". Technical Memorandum 295, 42 pp *[available through ECMWF, Reading, UK]*.

Van Genuchten M., 1980: "A closed-form equation for predicting the hydraulic conductivity of unsaturated soils". *Soil Sci. Soc. Amer. J.*, 44, 892\u2013898.

Viterbo P. and A. Beljaars, 1995: "An improved land surface parameterization scheme in the ECMWF model and its validation". Technical Report 75, 58 pp *[available through ECMWF, Reading, UK]*.

Viterbo P., 1996: "The representation of surface processes in General Circulation Models". PhD Thesis, 210 pp *[available through ECMWF, Reading UK]*.

Wagner, W., Lemoine, G. & Rott, H. (1999). A method for estimating soil moisture from ERS scatterometer and soil data, *Remote Sens. Environ*., 70, 191-207.